

## **General Disclaimer**

### **One or more of the Following Statements may affect this Document**

- This document has been reproduced from the best copy furnished by the organizational source. It is being released in the interest of making available as much information as possible.
- This document may contain data, which exceeds the sheet parameters. It was furnished in this condition by the organizational source and is the best copy available.
- This document may contain tone-on-tone or color graphs, charts and/or pictures, which have been reproduced in black and white.
- This document is paginated as submitted by the original source.
- Portions of this document are not fully legible due to the historical nature of some of the material. However, it is the best reproduction available from the original submission.

NASA CR-168029

GE R82AEB304



National Aeronautics and  
Space Administration

# BEARING FATIGUE INVESTIGATION III

by

A.H. Nahm  
E.N. Bamberger  
(General Electric)

and

H. Signer  
(Industrial Tectonics, Inc.)

General Electric Company

(NASA-CR-168029) BEARING FATIGUE  
INVESTIGATION 3 Final Report (General  
Electric Co.) 83 p HC A05/MF A01 CSCL 13I

N83-17880

Unclas  
G3/37 02541

Prepared for

National Aeronautics and Space Administration

NASA Lewis Research Center  
Contract NAS3-15337

ORIGINAL PAGE IS  
OF POOR QUALITY

1. Report No. NASA CR-168029		2. Government Accession No.		3. Recipient's Catalog No.	
4. Title and Subtitle Bearing Fatigue Investigation - III				5. Report Date May, 1982	
				6. Performing Organization Code	
7. Author(s) A.H. Nahm, <sup>(1)</sup> E.N. Bamberger, <sup>(1)</sup> H. Signer <sup>(2)</sup>				8. Performing Organization Report No. 82AEB304	
9. Performing Organization Name and Address (1) General Electric Co., Aircraft Engine Business Group, Cincinnati, OH (2) Industrial Tectonics, Inc., Bearing Division, Compton, California				10. Work Unit No.	
				11. Contract or Grant No. NAS 3-15337	
12. Sponsoring Agency Name and Address National Aeronautics Space Administration Washington, D.C. 20546				13. Type of Report and Period Covered Contractor Report	
				14. Sponsoring Agency Code	
15. Supplementary Notes Project Manager, Erwin V. Zaretsky, Bearings, Gearing and Transmission Group - Lewis Research Center, Cleveland, OH 44135					
16. Abstract This report documents the final segment of a comprehensive program performed by General Electric under NASA Contract NAS3-15337 to investigate and define the operating characteristics of large diameter rolling-element bearings in the ultra-high speed regimes expected in advanced turbine engines for high-performance aircraft.  In the first phase of the work reported herein, a high temperature lubricant, DuPont Krytox 143 AC, was evaluated at bearing speeds to 3 million DN. Compared to the results of earlier, similar tests using a MIL-L-23699 (Type II) lubricant, bearings lubricated with the high-density Krytox fluid showed significantly higher power requirements. Additionally, short bearing lives were observed when this fluid was used with AISI M50 bearings in an air atmosphere. The primary mode of failure was corrosion initiated surface distress (fatigue) on the raceways.  The second phase investigated the potential of a case-carburized bearing to sustain a combination of high-tangential and hertzian stresses without experiencing race fracture. Limited full scale bearing tests of a 120 mm bore ball bearing at a speed of 25,000 rpm (3 million DN) indicated that a carburized material could sustain spalling fatigue without subsequent propagation to fracture. Planned life tests of the carburized material had to be aborted, however, because of apparent processing-induced material defects.					
17. Key Words (Suggested by Author(s)) Bearings, High Temperature, High Speed, Lubrication, Carburizing, Fatigue, Corrosion			18. Distribution Statement Unclassified		
19. Security Classif. (of this report) Unclassified		20. Security Classif. (of this page) Unclassified		21. No. of Pages 77	22. Price* [REDACTED]

\* For sale by the National Technical Information Service, Springfield, Virginia 22161

## FOREWORD

This work was performed by the General Electric Company, Aircraft Engine Business Group, Cincinnati, Ohio under NASA Contract NAS3-15337. The NASA Project Manager was Mr. E.V. Zaretsky.

The authors would like to acknowledge the efforts of Mr. D. Kroeger of the General Electric M&PTL who was instrumental in coordinating the many facets of this program as well as performing the metallographic analysis of the CBS 600 material.

TABLE OF CONTENTS

<u>SECTION</u>		<u>PAGE</u>
1	Summary	1
	1.1 Background	1
	1.2 Task III - High Temperature, High Speed Lubricant Performance Tests	1
	1.3 Task IV - CBS 600 Bearing Tests	2
2	Introduction	3
3	Task III - High Speed, High Temperature Lubricant Performance Tests	5
	3.1 Introduction	5
	3.2 Experimental Data	5
	3.2.1 High Speed Bearing Tests	5
	3.2.2 Tester Modifications	9
	3.2.3 Test Bearings	10
	3.2.4 Test Lubricant	10
	3.2.5 Test Procedures	14
	3.3 Results & Discussion	14
	3.3.1 Parametric Study	14
	3.3.2 Bearing Life Evaluation	36
	3.3.3 Data Reliability and Ball Passing Frequency	43
	3.3.4 Additional Parametric Studies - Effect of Speed and Load	51
	3.4 Task III Conclusions	51
4	Task IV - CBS 600 Bearing Tests	59
	4.1 Introduction	59
	4.2 Test Bearings	59
	4.2.1 Induced Defect	64
	4.3 Results & Discussion	64
	4.3.1 Phase I - Fracture Demonstration Tests	64
	4.3.2 Phase II - Endurance Tests	69
	4.4 Task IV Conclusions	75
5	References	77

## LIST OF FIGURES

<u>Figure</u>		<u>Page</u>
1	High Speed Bearing Fatigue Test Facility	6
2	Three Million DN Bearing Fatigue Test Machine	7
3	High-Speed, High-Temperature Test Apparatus	8
4	Lubricant System for Test Bearings	8
5	ABEC-5 Grade Bearing for 3 Million DN Test Program	12
6	Viscosity as a Function of Temperature for Krytox 143 AC Lubricant	13
7	Bearing Temperatures vs. Inner Ring Path Oil Flow for Lube-to-Cooling Flow Ratios of 1/4.0	24
8	Bearing Temperatures vs. Inner Ring Path Oil Flow for Lube-to-Cooling Flow Ratios of 1/3.0	25
9	Bearing Temperatures vs. Inner Ring Path Oil Flow for Lube-to-Cooling Flow Ratios of 1/1.33	26
10	Bearing Temperatures vs. Inner Ring Path Oil Flow for Lube-to-Cooling Flow Ratios of 1/0	27
11	Bearing Temperatures vs. Inner Ring Path Coolant-to-Lube Ratios at a Total Coolant plus Lube Flow Rate of 126 cm <sup>3</sup> /sec.	28
12	Bearing Temperatures vs. Inner Ring Path Coolant-to-Lube Ratios at a Total Coolant plus Lube Flow Rate of 189 cm <sup>3</sup> /sec.	29
13	Bearing Temperatures vs. Inner Ring Path Coolant-to-Lube Ratios at a Total Coolant plus Lube Flow Rate of 221 cm <sup>3</sup> /sec.	30
14	Bearing Temperatures vs. Inner Ring Path Coolant-to-Lube Ratios at a Total Coolant plus Lube Flow Rate of 252 cm <sup>3</sup> /sec.	31
15	Bearing Power vs. Inner Ring Path Oil Flow at a Lube-to-Coolant Flow Ratio of 1/4.0	32

LIST OF FIGURES (CONTINUED)

<u>Figure</u>		<u>Page</u>
16	Bearing Power vs. Inner Ring Path Oil Flow at a Lube-to-Coolant Flow Ratio of 1/3.0	33
17	Bearing Power vs. Inner Ring Path Oil Flow at a Lube-to-Coolant Flow Ratio of 1/1.33	34
18	Bearing Power vs. Inner Ring Path Oil Flow at a Lube-to-Coolant Flow Ratio of 1/0	35
19	Bearing Power vs. Inner Ring Flow Path Coolant-to-Lubricant Flow Ratios for a Total Coolant plus Lube Flow Rate of 126 cm <sup>3</sup> /sec.	37
20	Bearing Power vs. Inner Ring Flow Path Coolant-to-Lubricant Flow Ratios for a Total Coolant plus Lube Flow Rate of 189 cm <sup>3</sup> /sec.	38
21	Bearing Power vs. Inner Ring Flow Path Coolant-to-Lubricant Flow Ratios for a Total Coolant plus Lube Flow Rate of 221 cm <sup>3</sup> /sec.	39
22	Bearing Power vs. Inner Ring Flow Path Coolant-to-Lubricant Flow Ratios for a Total Coolant plus Lube Flow Rate of 252 cm <sup>3</sup> /sec.	40
23	Inner Race Failure in Bearing S/N 116	44
24	Inner Race Failure in Bearing S/N 116	45
25	Overall View of Bearing S/N 118	46
26	Outer Race Failure in Bearing S/N 118	47
27	Cage for Bearing S/N 118	48
28	Balls from Bearing S/N 118	49
29	Ball Passing Acceleration-Frequency Spectrum for Bearings S/N 100 and S/N 116	50
30	Bearing Temperature vs. Load at Various Speeds	52

LIST OF FIGURES (CONTINUED)

<u>Figure</u>		<u>Page</u>
31	Inner Race Temperature vs. Speed at Various Loads	53
32	Outer Race Temperature vs. Speed at Various Loads	54
33	Bearing Power vs. Load at Various Speeds	55
34	Bearing Power vs. Speed at Various Loads	56
35	Massive Carbide Network in CBS 600 Inner Race After Carburizing at 940.6°C (1725°F) for 11 Hours	60
36	Microstructure of Carburized CBS 600 After a Diffusion Heat Treat Cycle at 982°C (1800°F) for 2 Hours in Vacuum	65
37	Microstructure of Carburized CBS 600 After a Diffusion Heat Treat Cycle at 1010°C (1850°F) for 2 Hours in Vacuum	66
38	Hardness Gradient in CBS 600 After Carburization and 1010°C (1850°F) Diffusion Heat Treatment in Vacuum for 2 Hours	67
39	Premature Inner Race Failures in Bearing S/N 5 After 0.65 Hours Testing - (Failures did not occur at the induced defect.)	68
40	Overall View of Failed Bearing S/N 2 which was Operated for 24.7 Minutes After Spalling Failure	70
41	CBS 600 Inner Race of Bearing S/N 2 After Extended Running Following Initial Spalling Failure	71
42	Typical Spalling Fatigue Failure on CBS 600 Inner Rings on Bearing S/N 3	72
43	Typical Spalling Fatigue Failure on CBS 600 Inner Rings on Bearing S/N 4	73
44	Cross Sectional View of Cracks in CBS 600 Inner Races from Bearing S/N 6	74

LIST OF TABLES

<u>Table</u>		<u>Page</u>
I	Chemical Analysis of Vacuum Induction, Consumable-Electrode Vacuum Remelted AISI M50 Bearing Steel	11
II	Typical Properties of Krytox 143 AC Polymeric Perfluorinated Oil	11
III	Matrix of Test Conditions for Parametric Study	15
IV	Test Data Sheets for Bearings Tested at Constant Load, Constant Speed and Varying Oil Flow Rates	16
V	Test Data Sheets for Bearings Tested at Constant Oil Flow and at Variable Loads and Speeds	20
VI	Summary of Bearing Tests, Test Life and Post-Test Condition	41
VII	Nominal Chemical Composition of CBS 600	61
VIII	Forging Procedures for CBS 600 Bearing Races	62
IX	Heat Treating Procedure for CBS 600	63

**PRECEDING PAGE BLANK NOT FILMED**

## SECTION 1 SUMMARY

### 1.1 BACKGROUND

General Electric, under NASA contract, has been conducting a program to explore and define the operating characteristics of large diameter rolling-element bearings, in the ultra-high speed regimes expected in the engines for advanced, high performance aircraft. This final report deals with a portion of Task III and all of Task IV of the subject program. Earlier tasks, as well as a portion of Task III, have been documented in various reports issued during the life-span of this contract (1-9)\*.

### 1.2 TASK III - HIGH TEMPERATURE, HIGH SPEED LUBRICANT PERFORMANCE TESTS

This portion of Task III was designed to evaluate the effect of a developmental high temperature lubricant on the operating characteristics of rolling-element bearings at speeds to 3 million DN. In earlier, similar high speed bearing tests (7, 8 and 9), a commercial Type II synthetic lubricant was used.

Following the procedure used in these earlier tests, a parametric study was conducted using 120 mm bore, split inner ring AISI M-50 bearings and a polymeric perfluorinated fluid, marketed by DuPont under the trade name, Krytox 143 AC.

During the first series of parametric tests with the Krytox fluid, the inner race speed was held constant at 25,000 rpm ( $3.0 \times 10^6$  DN), the thrust load was 22,240 Newtons (5,000 lbs.) and the oil inlet temperature was maintained at 166°C (330°F). The bearings were lubricated through passages at the inner ring split, and the exterior bearing surfaces were cooled with an independently adjustable oil flow. Bearing ring temperatures and power demand were measured for a variety of lubricant and cooling oil flows.

In the second series of tests, the lubricant and cooling oil flows were held constant at values which produced the most favorable bearing performance during the first series of tests. With the oil inlet temperature adjusted to achieve 288°C (550°F), inner and outer ring temperatures, speeds and loads were varied from 12,000 ( $1.44 \times 10^6$  DN) to 25,000 rpm ( $3 \times 10^6$  DN) and from 6,672 to 22,240 Newtons (1,500 to 5,000 lbs.), respectively.

The results can be summarized as follows:

- Practical limits were established for the range of lubricant flow to the test bearings. Low flow rates produced bearing temperatures beyond the upper, acceptable limit. High flow rates increased the bearing power demand beyond the capacity of the test rig drive motor.

\* Numbers in parentheses refer to references.

- Bearing race temperatures, temperature gradients across the bearings and power losses could be tuned and varied with load, with speed and with both lubricant flow rate into the bearings and cooling flow to the inner races.
- Cooling oil flow to the outer races affected the outer race temperatures significantly, but had only a small effect on the inner race temperatures. The power losses due to changes in cooling oil flow to the outer race were insignificant.
- Compared with the results of tests using a type II oil, the high density Krytox lubricant had a significant effect on the power requirements.
- Short bearing life was obtained in bearing tests with the Krytox 143 AC in an air atmosphere. The primary mode of failure was corrosive surface fatigue occasioned by pitting on the bearing raceway surfaces.

### 1.3 TASK IV - CBS 600 BEARING TESTS

This task was intended as a preliminary evaluation of the ability of a carburized bearing to sustain the high tangential stresses of high DN bearings without experiencing the catastrophic failure mode observed earlier (9) with VIM-VAR\* M50.

To accomplish this, inner races were manufactured using a case-carburizing alloy (CBS 600) and assembled into 120 mm bore split-inner-ring ball bearings. The outer rings were VIM-VAR M50. The bearings were installed in the high speed, high temperature fatigue tester and were run at 25,000 rpm ( $3 \times 10^6$  DN) with a thrust load of 22,240 Newtons (5,000 lbs.). A bearing race temperature of 216°C (420°F) was maintained. These test conditions were identical to those used in the previous tests with the AISI M50 bearings.

In the fracture demonstration tests, an artificial defect was introduced in the CBS 600 inner race. Again, these tests were conducted under identical conditions as those reported in (9). The results of the current tests indicated that an inner race, manufactured of a case carburized material, can withstand continued operation without fracturing after a fatigue spall failure has developed in its raceway at high speeds and under high loads.

However, during subsequent life-tests of CBS 600 inner races, extremely short lives of less than 4 hours were encountered. Thus, while the material demonstrated its potential resistance to fracture, the results are somewhat clouded by apparent processing defects resulting from the carburizing/heat-treat cycle. The test results must therefore be viewed in this context.

\* Vacuum Induction Melted - Vacuum Arc Melted

## SECTION 2 INTRODUCTION

Rolling-element bearings for advanced technology aircraft engines are expected to operate at speeds to 3 million DN (DN is the product of the bearing bore in millimeters and the shaft speed in rpm). Current production engine bearings operate at speeds less than 2.3 million DN. Additionally, bearing temperatures for these advanced engines could go above the current 218°C (425°F) maximum operating levels. Because compressor or turbine blade tip speeds and disk burst strengths begin to limit the maximum speed of rotating components, a bearing speed of 3 million DN appears to be the practical limit of aircraft engine operation.

General Electric, under NASA contract, has been conducting a long term program to explore and define the operating characteristics of large diameter rolling-element bearings in the ultra-high speed regimes expected in the engines for advanced, high performance aircraft.

The prime objective of the program was to obtain design information relating the effect of high rotational speeds, up to 25,000 rpm,  $3 \times 10^6$  DN, on the fatigue life, thermal behavior, lubrication characteristics, and operational conditions, of main-engine size rolling-element bearings.

Comprehensive, controlled full-scale 120 mm bearing tests have been conducted under conditions of load, temperature and environment typical of those expected in advanced aircraft engines. Consequently, the data and information being generated are directly applicable to the design of bearings for advanced high speed aircraft gas turbine engines.

During the term of this contract, a number of modifications were made. These resulted from a continuing effort between GE and NASA to achieve a maximum yield and efficiency from the program. The generic program was divided into the following tasks:

- Task I - Bearing and Lubricant Procurement
- Task II - Test Rig Design and Fabrication
- Task III - Fatigue Tests
- Task IV - CBS 600 Bearing Tests

In Task III, Fatigue Tests, over 185,000 hours of 120 mm ball bearing tests were accumulated, including more than 75,000 hours at 3 million DN. From this activity, the ability to successfully operate large diameter bearings at ultra-high DN values was demonstrated. In addition, ring fracture, a potentially critical failure mode in high speed bearings, was identified and the effect of it on bearing integrity was demonstrated in controlled tests.

Because of the time span covered by this contract, the earlier test results (Task I, II and portions of III) have been reported in the open literature (Ref. 1-9). Consequently, this report deals only with the last portion of Task III - High Temperature, High Speed Lubricant Performance Evaluation and Task IV - CBS 600 Bearing Tests.

SECTION 3  
TASK III - HIGH SPEED, HIGH TEMPERATURE LUBRICANT PERFORMANCE TESTS

3.1 INTRODUCTION

As reported in reference (9), over 150,000 bearing test hours were accumulated with two groups of thirty each, 120 mm bore split-inner-ring ball bearings, operating at 1.44 and 3.0 million DN at 221°C (430°F) and using a type II oil. This fatigue test program was preceded by a parametric study reported in reference (7). The effects of lubricant flow for various lubrication and cooling techniques were investigated, resulting in essential information for the successful operation of bearings at high speeds.

The data of the high-speed, high-temperature bearing performance tests reported herein supplement those of the earlier parametric study since they were collected on the same test apparatus and with the identical type test bearings. Applying the lubrication techniques of the earlier program, bearing performance was measured at temperatures to 288°C (550°F) with Krytox 143 AC. Even though only short bearing lives were achieved, the test results are of considerable engineering value as they illustrate the significant effects that a lubricant has on the performance of high speed bearings.

3.2 EXPERIMENTAL DATA

3.2.1 High Speed Bearing Tester

The test machines used in this program are identical to those used for the  $1.44 \times 10^6$  DN and  $3 \times 10^6$  DN tests used in earlier programs. Figures 1 and 2 are overall photographs of the high speed testers.

A schematic of the high speed, high temperature bearing tester is shown in Figure 3. The tester consists of a shaft to which two test bearings are mounted. Loading is applied through ten springs which give a thrust load to the bearings. Dual flat belts are used to drive the test spindle from a 75 kW (100 hp) fixed speed electric motor. The drive motor is mounted to an adjustable base so that drive pulleys can be used for 12,000 to 25,000 rpm with the same drive belts. The drive motor is controlled by a reduced voltage autotransformer starter which permits a selection of the motor acceleration rate during startup. This control protects the bearings from undesirable acceleration during startup.

The lubrication system delivers up to  $473 \text{ cm}^3/\text{sec}$ . (7.5 gallons per minute) to the test rig. There are two lubricant loops in the system. The oil flow in each loop is adjusted by flow control valves and can be individually measured by a flow rate meter without interrupting the machine operation, as shown in Figure 4. The first loop supplies cooling oil to each bearing outer race and is designated  $C_0$ . The second loop is divided by a lubricant manifold which feeds individual annular grooves or channels at the shaft internal diameter, proportioning the amount of oil which is to lubricate and/or cool the inner race.  $L_i$  designates the oil flow to the bearing through a plurality of radial

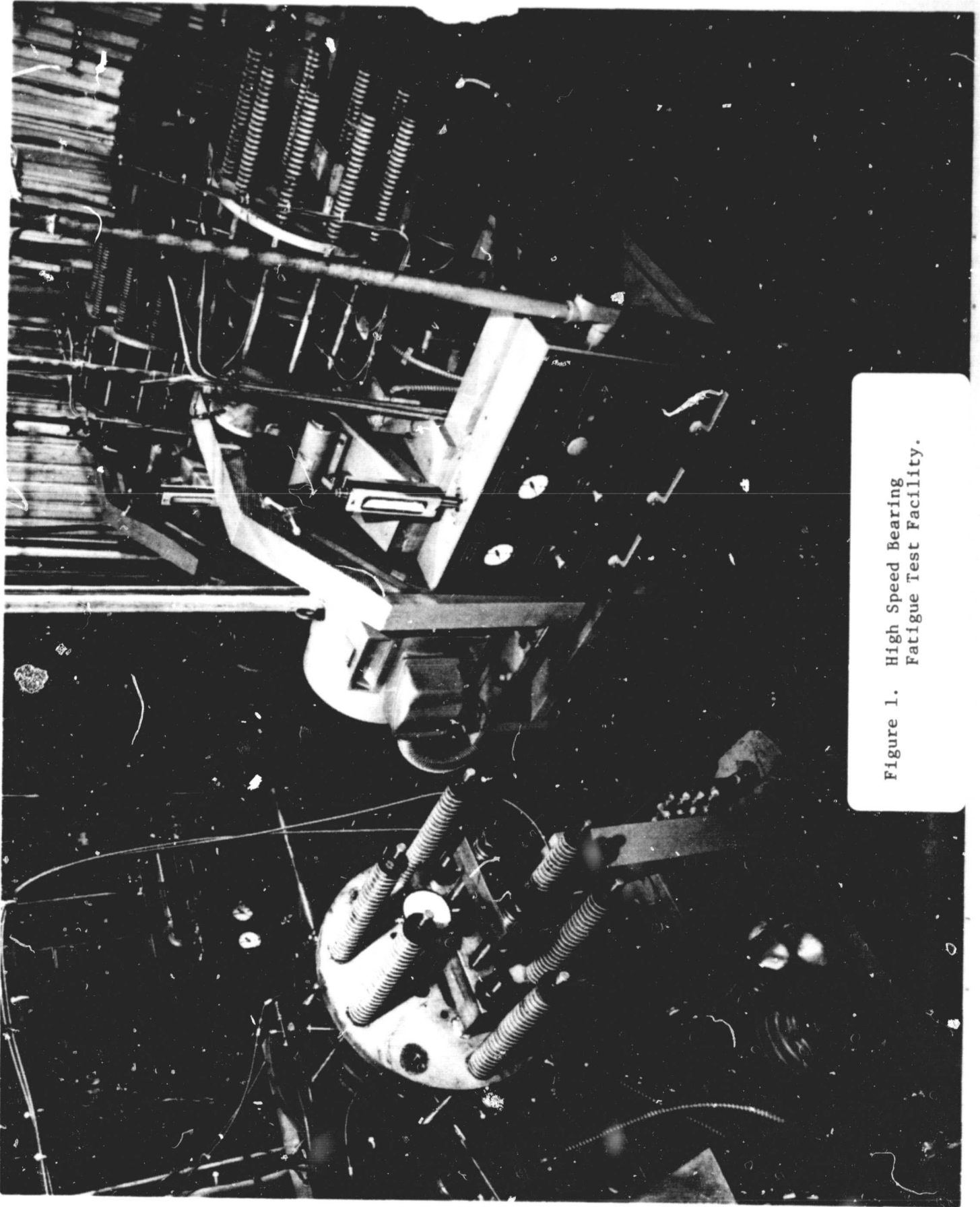


Figure 1. High Speed Bearing Fatigue Test Facility.

ORIGINAL PAGE  
BLACK AND WHITE PHOTOGRAPH

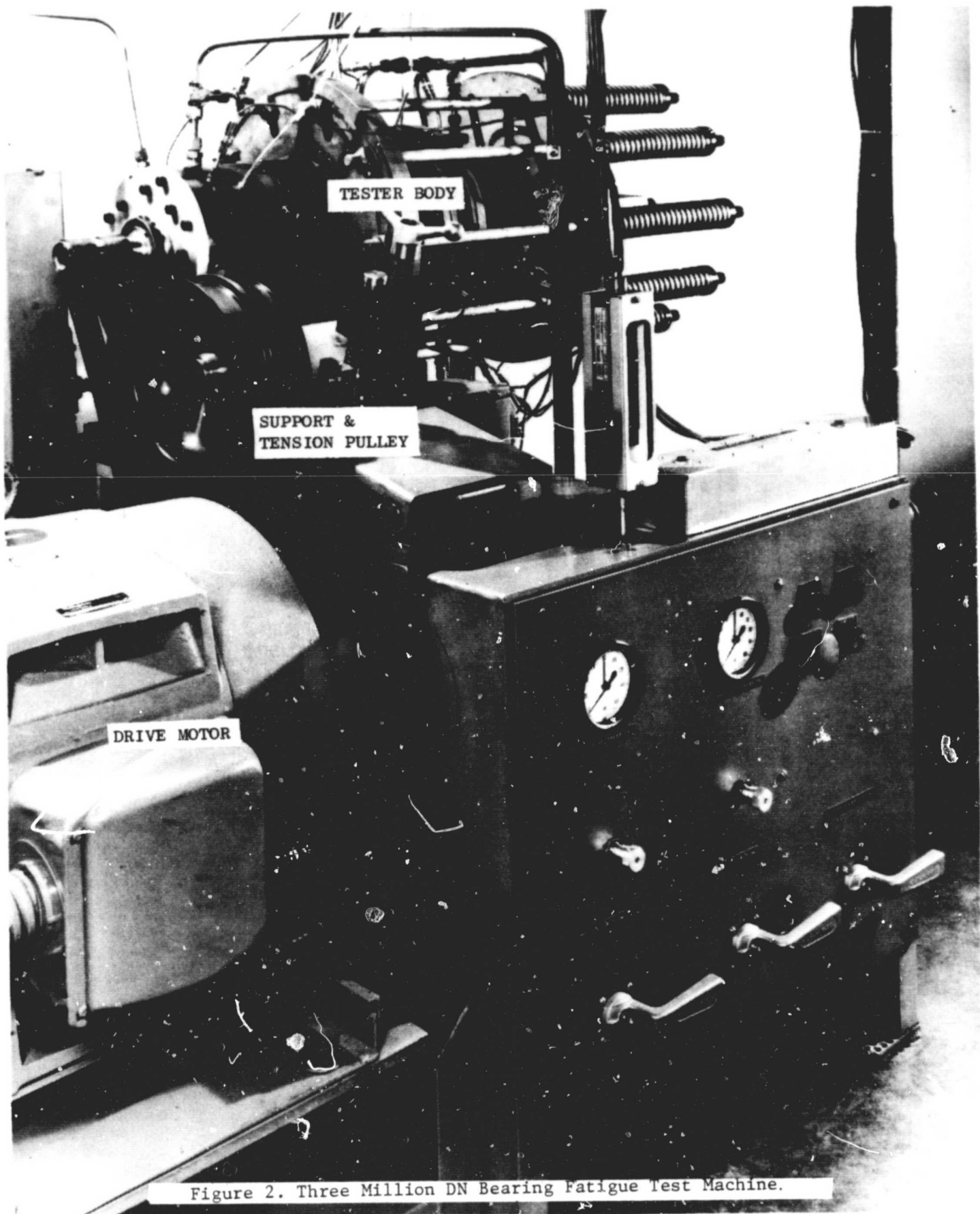


Figure 2. Three Million DN Bearing Fatigue Test Machine.

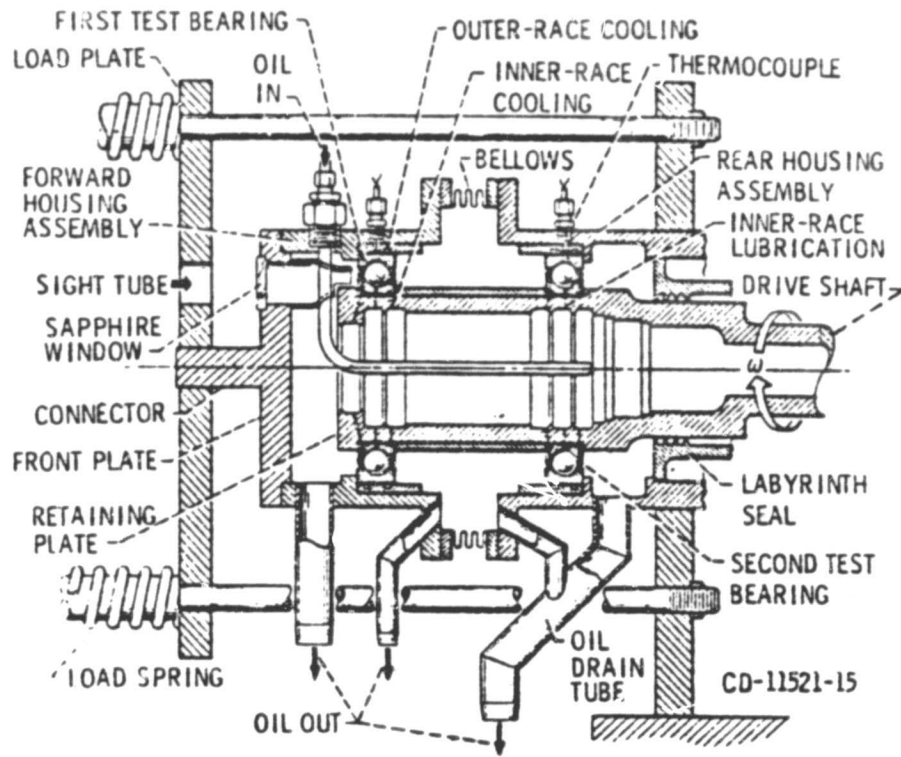


Figure 3. High-Speed, High-Temperature Test Apparatus.

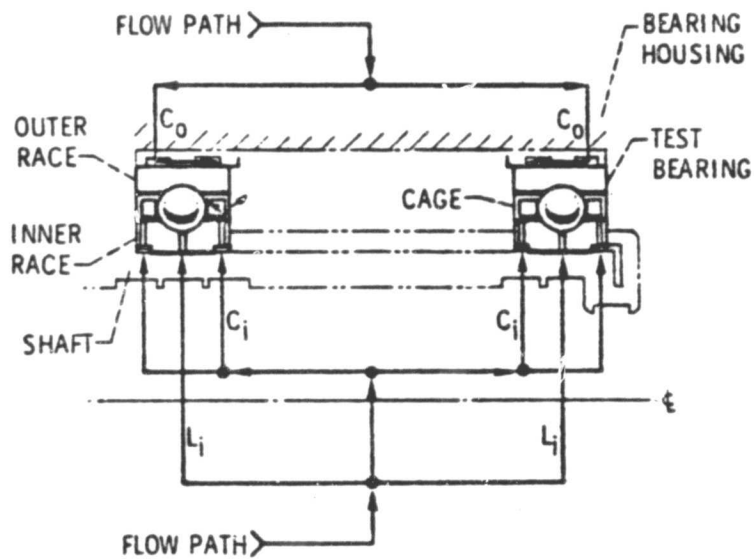


Figure 4. Lubricant System for Test Bearings.

passages at the inner-race split.  $C_i$  designates the lubricant supply to the inner race land/cage interface. The lubricant system permits a selection of various lubricant schemes. These include bearing lubrication through the inner-race split, lubrication of the cage-race shoulder contact region, the application of inner and/or outer-race cooling, and a selection of any desired flow ratio for cooling and lubrication as well as the conventional lubrication through jets.

By means of the system of valves and manifolds previously discussed, an unlimited number of combination of oil flows can be achieved to evaluate various conditions. Consequently, values of  $L_i$ ,  $C_i$  and  $C_o$  can be controlled independent of each other. A third lubricant loop adapted from an adjacent machine supplies an ester base type II oil to the slave bearing which supports the shaft; this is not shown in Figures 3 and 4.

The instrumentation includes the standard protective circuits which shut down a test when a bearing failure occurs, or when any of the test parameters deviate from the programmed conditions. Measurements were made of bearing inner and outer-race and lubricant temperatures, and machine vibration level. Speed and spindle excursion measurements were made with proximity probes and displayed by numerical read-out and oscilloscope, respectively. The oil flow was established by a flowmeter, and bearing outer-race and lubricant inlet and outlet temperatures were measured by thermocouples and continuously recorded on a strip chart recorder. The inner-race temperature of the front test bearing was measured with an infrared pyrometer.

### 3.2.2 Tester Modifications

Due to the known corrosive nature of the Krytox 143 AC lubricant at operating temperatures, it was required to incorporate several modifications to the high-speed bearing tester selected for testing with this lubricant.

The lubricant circuit was completely rebuilt with a new pump, valves, flow meters, high capacity heat exchangers and oil filters. New external outer ring cooling lines were installed to insure adequate drainage of the test bearing chambers. All the new components were either constructed of stainless steel or were electroless nickel plated. To facilitate machine startup with the high viscosity Krytox as well as to maintain lube temperatures under all operating conditions, a heater was added to the lube reservoir.

All test rig surfaces exposed to the lubricant were electroless nickel plated to a thickness of  $7.62 \times 10^{-3}$  mm (.0003 inch) minimum. The support bearing and its cavity remained unchanged. This bearing was lubricated with type II oil from an adjacent machine. Contamination of the Krytox test fluid with type II oil was prevented by adding a slinger to the shaft mid-section. The intermediate section of the test rig, located between two labyrinth seals, was continuously drained and any fluid leaking into this cavity was discarded.

A direct reading power meter was added to the electrical system to improve the accuracy and efficiency of the drive power measurements.

Certain features of the original machine were sacrificed. The probes used to sense cage speed and radial spindle excursion have a temperature limit of 221°C (430°F). Therefore, spindle excursion was measured only near the support bearing and cage speed measurement was eliminated. Spindle speed was measured with a probe located near the support bearing.

### 3.2.3 Test Bearings

The test bearings were ABEC-5 grade, split-inner-race 120 mm bore ball bearings. The inner and outer races, as well as the balls, were manufactured from one heat of vacuum-induction melted, vacuum-arc remelted AISI M50 steel. The chemical analysis of the specific VIM-VAR M50 heat is shown in Table I. The nominal hardness of the balls and races was Rockwell C 63 at room temperature. Each bearing contained 15 balls, each 2.0638 cm (13/16 in.) in diameter. The bearings were assembled to have a nominal 23° contact angle. The cage was a one-piece inner-land riding type, made out of an iron base alloy, AMS 6415, heat-treated to a Rockwell C hardness range of 28 to 35 and having a 0.005 cm (0.002 in.) maximum thickness of electroless nickel plate per specification AMS 2404. The cage balance was 3 gm-cm (0.042 oz-in.). The retained austenite content of the ball and race material was less than 3 percent. The inner and outer-race curvatures were 54 and 52 percent, respectively. All components with the exception of the cage were matched within ± one Rockwell C point. Surface finish of the balls was 2.5 µcm (1 micro in.) AA, and the inner and outer raceways were held to a 5 µcm (2 micro in.) AA maximum surface finish.

An outline drawing of the test bearing is shown in Figure 5. The bearing design permitted under-race lubrication by virtue of radial grooves machined into the halves of the split inner races. Provision was also made for inner-race land-to-cage lubrication by the incorporation of several small diameter holes radiating from the bore of the inner race to the center of the inner-race shoulder.

### 3.2.4 Test Lubricant

The oil used for the parametric studies is marketed by DuPont under the trade name Krytox 143 AC. It is a polymeric perfluorinated fluid with an average molecular weight approaching 7000.

The oil is an odorless and colorless, completely fluorinated organic polymer. It is quite resistant to heat, either alone or in the presence of oxygen, and will slowly decompose above 399°C (750°F). The major properties of the oil are presented in Table II and temperature-viscosity curve is shown in Figure 6. This lubricant has been studied by several laboratories. The Air Force Materials Laboratory, Wright-Patterson AFB, Ohio has conducted a series of extensive investigations on this fluid (10 and 11). Because this lubricant had been stored for some time at the General Electric Company, a sample was sent to DuPont for an analysis verification. DuPont reported that the fluid met all original chemical and physical property requirements.

ORIGINAL PAGE IS  
OF POOR QUALITY

TABLE I

Chemical Analysis of Vacuum Induction, Consumable-Electrode  
Vacuum Remelted AISI M50 Bearing Steel

<u>Element</u>	<u>Composition of Races and Balls, wt.%</u>
Carbon	0.83
Manganese	0.29
Phosphorus	0.007
Sulfur	0.005
Silicon	0.25
Chromium	4.11
Molybdenum	4.32
Vanadium	0.98
Iron	Balance

TABLE II

Typical Properties of Krytox 143 AC Polymeric Perfluorinated Oil

Viscosity, centistokes at	-13°C (0°F)	33,000
	38°C (100°F)	270
	99°C (210°F)	26
	204°C (400°F)	3.9
	260°C (500°F)	2.1
Viscosity Index, ASTM D2270		134
Pour Point, °C ASTM D92		-34
Thermal Conductivity BTU/hr. (ft) <sup>2</sup> (°F/ft)	149°C (300°F)	0.051
	260°C (500°F)	0.051
Density, grams/ml at	99°C (210°F)	1.77
	204°C (400°F)	1.59
Specific Heat, BTU/lb/°F at 99°C (210°F)		.252
Volatility D972 Mod. wt % loss, 6-1/2 hours at	204°C (400°F)	1.0
	at 260°C (500°F)	4.0

ORIGINAL PAGE 13  
OF POOR QUALITY

- RINGS AND BALLS**
- M-50 (VIM-VAR), Rc 62-64
  - 15 BALLS, 13/16 DIA
  - $f_0 = 52\%$ ,  $f_1 = 54\%$
  - BALLS: 1 AA
  - RACEWAYS: 2 AA
  - CONTACT ANGLE:  $23^\circ$

- SEPARATOR**
- AMS 6415, Rc 28-35
  - NICKEL PLATED TO AMS 2404
  - BALANCED TO 3 GM-CM

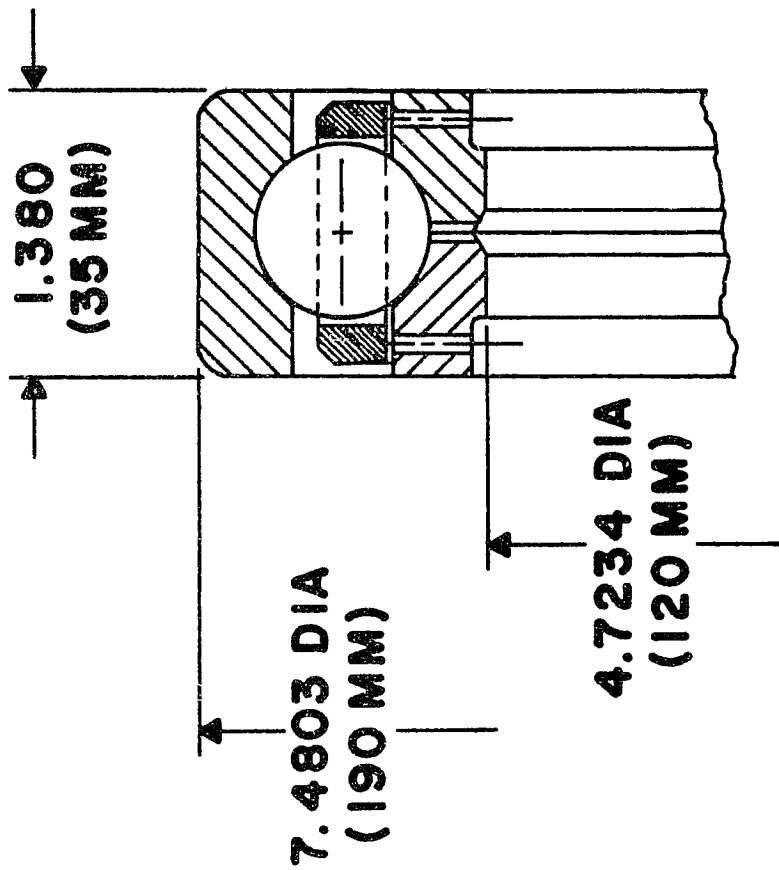


Figure 5. ABEC-5 Grade Bearing for 3 Million DN Test Program.

ORIGINAL PAGE IS  
OF POOR QUALITY

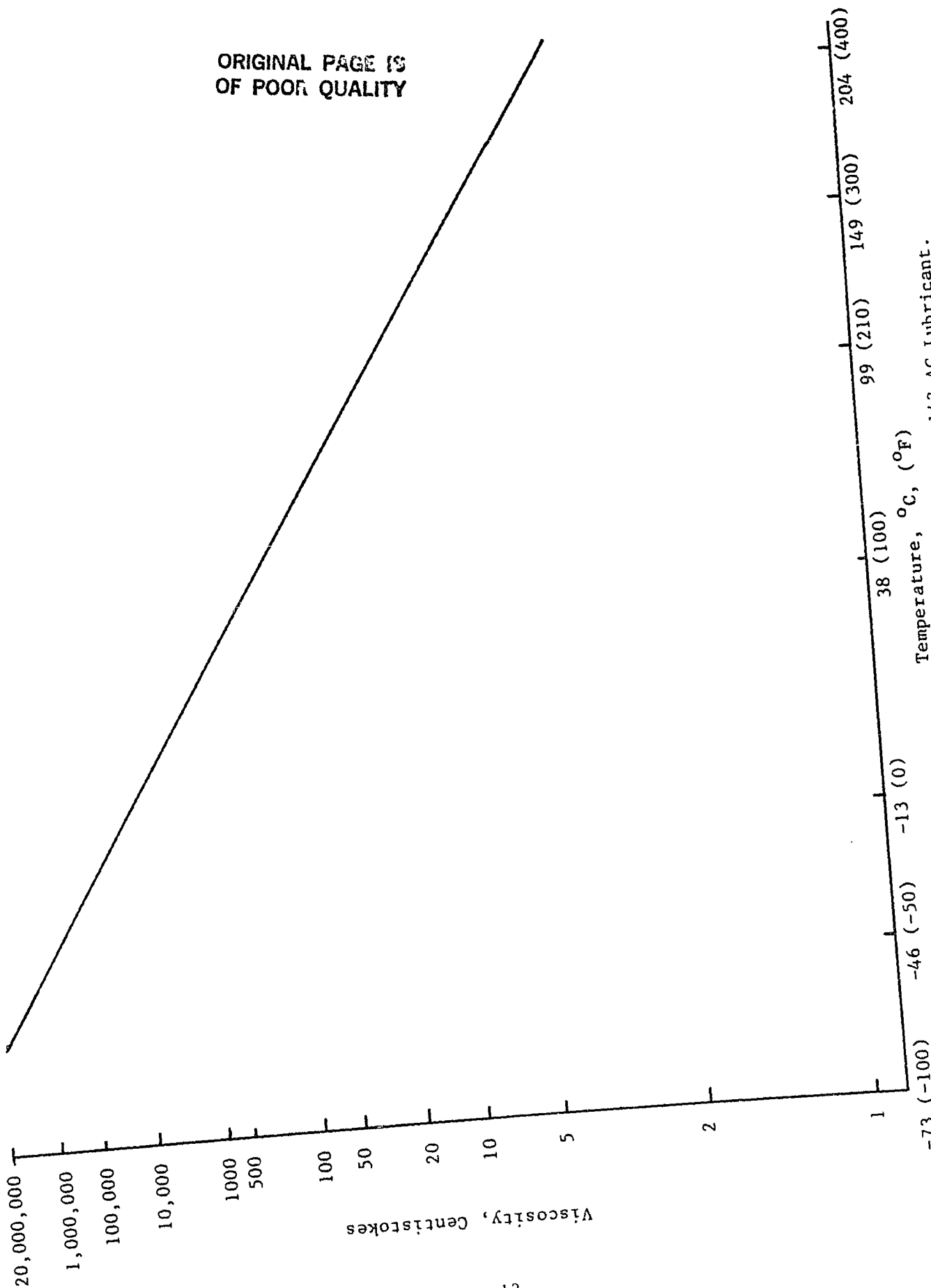


Figure 6. Viscosity as a Function of Temperature for Krytox 143 AC Lubricant.

Prior to testing, the fluid was circulated through filters for over 30 hours. A sample check after the filtration showed an acceptable count of contamination particles.

The oil used for the support bearing was a 5 centistoke neopentylpolyol tetraester. This is a type II oil qualified to MIL-L-23699.

### 3.2.5 Test Procedures

The initial objective of the study was to collect data on the performance of ball bearings at speeds to three million DN with ring temperatures to 316°C (600°F), using Krytox 143 AC as a lubricant. Following this, tests were to be run for direct comparison with earlier tests run with a type II oil, MIL-L-23699.

Additionally, tests were to be conducted to find the optimum operating conditions at 25,000 rpm with 22,240 Newtons (5,000 lbs.) thrust load and 316°C (600°F) test bearing operating temperature, followed by tests under the same lube flow conditions at lower speeds and loads.

During the initial testing with maximum bearing temperatures of 316°C (600°F) and maximum oil inlet temperatures of 204°C (400°F), an increase in the machine vibration and a "rough hand feel" of the shaft suggested some deterioration of the test bearings. Inspection revealed that the raceways were severely pitted. There were signs of corrosive attack and surface distress on the balls; and severe wear was observed at the separator ball pockets and moderate wear at the separator lands. To reduce these corrosive effects of the Krytox, it was decided to modify the test conditions.

Consequently, the parametric tests were rescheduled to operate at a maximum ring temperature of 288°C (550°F) and a maximum oil inlet temperature of 166°C (330°F). The latter was necessary to stay within the power limitations of the drive motor. A matrix of the test conditions is shown in Table III.

## 3.3 RESULTS AND DISCUSSION

### 3.3.1 Parametric Study

The effects of lubricant and cooling oil flow rates on bearing temperatures and power requirements were determined, and the results are presented in Tables IV and V. The data has been plotted to determine the consistency and accuracy of the results and to show the major trends of bearing performance.

For correlation with the raw data presented in this report, all graphs are illustrated in terms of total flow in the lubricant loops, i.e., "Outer Race Flow" and "Oil Flow, Inner Race Path", representing total flow supplied by the machine to both test bearings.

The tests in the parametric study are based on the following operating conditions:

Speed	-	25,000 rpm ( $3 \times 10^6$ DN)
Thrust load	-	22,240 Newtons (5,000 lbs.)
Lube oil	-	Krytox 143 AC
Lube inlet temperature	-	166°C (330°F)

TABLE III

Matrix of Test Conditions for Parametric Study

Inner Ring Flow Ratio $C_i/L_i$	$C_i + L_i$ , $\text{cm}^3/\text{sec.}$ (gpm)	Outer Ring Flow, $\text{cm}^3/\text{sec}$ (gpm)				
		32 (0.5)	63 (1.0)	126 (2.0)	189 (3.0)	221 (3.5)
0	189 (3.0)		#	✓	✓	
	126 (2.0)			✓	#	
	63 (1.0)			✓	#	
1.33	189 (3.0)		#	✓	✓	
	126 (2.0)			#	✓	
	63 (1.0)				#	
3.0	252 (4.0)	#	✓	✓	✓	
	221 (3.5)			✓	✓	✓
	189 (3.0)		#	✓	✓	
	126 (2.0)			#	✓	
4.0	252 (4.0)	#	✓	✓	✓	
	221 (3.5)		#	✓	✓	✓
	189 (3.0)		#	✓	✓	
	126 (2.0)			#	✓	

✓ Successful test with  
temperature data

# Shut-down, temperature  
limit reached

□ Unsafe area; did not  
run

All flows indicate total  
machine flow, i.e., for two  
test bearings.



TABLE IV (CONT'D.). Test Data Sheets for Bearings Tested at Constant Load, Constant Speed and Varying Oil Flow Rates.

PERFORMANCE TEST LOG  
 HIGH SPEED BALL BEARINGS  
 WITH PR 143AC LUBRICANT W.O. 7001-7

TEST BRG. P/N: 13052 MOD FRONT BRG. S/N 105 REAR BRG. S/N 109  
 LI/C: 1/1.33 (JET #2)

• TEST PARAMETER (VARIABLE)  
 Δ TEST CONDITIONS (FIXED)  
 \*\* CALCULATED VALUES

TEST NO.	BEARING LOAD (LBS)	SPINDLE SPEED (RPM)	OIL FLOW (GPM)			TEMPERATURES (°F)												SHAFT EXCURSION TIR (INCH)	VIB. LEVEL (1)	MOTOR POWER (KW)	NOTES	BY DATE	
			LI **	I/R PATH	CO **	O/R PATH	FRONT BEARING	REAR BEARING	SUPPORT BRG	ILX OUT	OIL IN	OIL OUT	CO OUT	O/R	O/R	CO OUT	OIL IN						OIL OUT
1-2-6-6	5000	25000	.64	3.0	1.5	3.0	530	329	540	524	389	531	515	523	372	496	258	44	386	16	84	GAGE PRESS 28.5	W/B
		24,615		70		70													43			SURGES (FOR PUBLIC)	B2/PA
1-2-6-4	5000	25000	.64	3.0	1.0	2.0	528	329	549	546	404	532	524	530	383	490	258	43	382	33	84	GAGE PRESS 29 PSI	W/B
		24,515		70		43													45				B 2/78
1-2-4-6	5000	25000	.43	2.0	1.5	3.0	538	329	559	550	367	524	538	521	367	496	260	134	354	16	72	REAR BEARING SURGES	W/B
		24,840		43		70													27				5/17/78



ORIGINAL PAGE IS  
OF POOR QUALITY

TABLE IV (CONT'D.). Test Data Sheets for Bearings Tested at Constant Load,  
Constant Speed and Varying Oil Flow Rates.

PERFORMANCE TEST LOG  
HIGH SPEED BALL BEARINGS  
WITH PR 143AC LUBRICANT

W.O. 7001-7

TEST BRG. P/N: 13052 MOD.  
Li/Cr 1/4.0 (JET # 4)

FRONT BRG. S/N 0100  
REAR BRG. S/N 0116  
EXCEPT AS NOTED BELOW  
SEE NOTES

\* TEST PARAMETER (VARIABLE)  
△ TEST CONDITIONS (FIXED)  
\*\* CALCULATED VALUES

TEST NC.	BEARING LOAD (LBS)	SPINDLE SPEED (RPM)	OIL FLOW (GPM)				TEMPERATURES (*F)												SUBPRT BRG. OIL IN	SUBPRT BRG. OIL OUT	INLET EXCURSION TIR (INCH)	VIB. LEVEL (%)	MOTOR POWER (KW)	NOTES	BY DATE
			L1 **	I/R PATH	Co **	O/R PATH	FRONT BEARING		REAR BEARING		OIL INLET		FRONT BEARING		REAR BEARING		OIL OUT								
							O/R	Co	O/R	Co	O/R	Co	O/R	Co	O/R	Co	O/R	Co							
1-4-8-6	5000	25,000	.4	4.0	1.5	3.0	492	504	507	380	470	498	507	367	468	258	145	385	18	87	GAGE PRESS 2.9 PSI	W/B	8-15-78		
		24,530		9.5		7.0												55	5.0						
1-4-8-4	5000	25,000	.4	4.0	1.0	2.0	492	513	518	393	470	508	516	378	467	257	144	384	2.5	88	GAGE PRESS 2.9 PSI	W/B	8-15-78		
		24,510		9.5		4.3												42	4.6						
1-4-8-2	5000	25,000	.4	4.0	.5	1.0	488	532	537	418	468	538	543	430	473	257	143	381	1.8	85.5	GAGE PRESS 2.9 PSI	W/B	8-15-78		
		24,565		9.5		2.0												55	4.7						
1-4-7-7	5000	25,000	.35	3.5	1.75	3.5	500	510	510	379	481	500	510	366	473	258	141	378	2.4	82.5	GAGE PRESS 1.9 PSI	W/B	8-15-78		
		24,575		82		82												42	4.2						
1-4-7-6	5000	25,000	.35	3.5	1.5	3.0	499	513	513	382	480	503	514	369	474	258	142	378	2.3	82	GAGE PRESS 1.9 PSI	W/B	8-15-78		
		24,565		82		70												44	3.8						
1-4-7-4	5000	25,000	.35	3.5	1.0	2.0	499	525	525	396	480	517	526	380	475	260	143	377	2.4	81.5	GAGE PRESS 1.9 PSI	W/B	8-15-78		
		24,565		82		4.3												42	4.5						
1-4-6-6	5000	25,000	.3	3.0	1.5	3.0	510	541	537	390	512	520	529	375	492	262	135	376	2.6	79	GAGE PRESS 12.5 PSI BEARING TEST F-110 R-120	W/B	8-15-78		
		24,810		70		70												30	2.6						
1-4-6-4	5000	25,000	.3	3.0	1.0	2.0	510	560	554	410	512	535	545	392	492	264	136	371	2.6	80	GAGE PRESS 1.9 PSI BEARING TEST F-110 R-120	W/B	8-15-78		
		24,780		70		4.3												30	2.2						
1-4-4-6	5000	25,000	.2	2.0	1.5	2.0	522	555	549	381	515	552	538	399	500	260	132	351	2.9	66	GAGE PRESS 7.5 PSI BEARING TEST F-118 R-108	W/B	8-15-78		
		25,000		4.3		70												30	2.5						

ORIGINAL PAGE IS  
OF POOR QUALITY

TABLE V. Test Data Sheets for Bearings Tested at Constant Oil Flow  
and at Variable Loads and Speeds.

PERFORMANCE TEST LOG  
HIGH SPEED BALL BEARINGS  
WITH PR 143AC LUBRICANT W.O. 7001-7

TEST BRG. P/N: 23052 MAG. FRONT BRG. S/N 0100 \* TEST PARAMETER (VARIABLE)  
LI/GI 1/30 (JET#3) REAR BRG. S/N 0116 Δ TEST CONDITIONS (FIXED)  
\*\* CALCULATED VALUES

TEST NO.	BEARING LOAD (LBS)	SPINDLE SPEED (RPM)	OIL FLOW (GPM)			TEMPERATURES (°F)												SHAFT EXCURSION TIR (INCH)	VIB. LEVEL (%)	MOTOR POWER (KW)	NOTES	BY DATE		
			LI **	I/R PATH	Co **	O/R PATH	FRONT BRG. I/R	OIL INLET	FRONT BEARING O/R	FRONT BEARING Co	OIL OUT	REAR BEARING O/R	REAR BEARING Co	OIL OUT	SLEWING BRG O/R	SLEWING BRG OIL IN	Hx OUT							
3-1-17	5000	25000	.25	2.0	175	3.5	545	340	554	547	397	524	539	552	389	517	259	133	356	.0017	2.5	66.5	GAGE PRESS 11.25 PSI	AD 8-3-78
	5000	24880		4.3		82														33	2.3			
3-2-47	3000	25000	.25	2.0	175	3.5	526	340	535	528	395	517	521	530	386	508	260	134	342	.0020	2.6	60	GAGE PRESS 11 PSI	AD 8-3-78
	2900	24970		4.3		82														40	2.7			
3-3-47	1500	25000	.25	2.0	175	3.5	506	340	525	518	392	511	503	514	382	496	260	133	333	.0020	3.2	56	115 psi Gage	AD 8-3-78
	1500	25010		4.3		82														40	2.6			
3-4-47	5000	20850	.25	2.0	175	3.5	490	341	507	503	390	478	494	505	382	471	234	125	320	.0019	1.4	49.5	GAGE PRESS 11.25 PSI	AD 8-3-78
	5000	20740		4.3		82														38	2.6			
3-5-47	3000	20850	.25	2.0	175	3.5	475	340	489	484	386	468	473	482	378	455	233	125	302	.0020	1.4	44	GAGE PRESS 11.5 PSI	AD 8-3-78
	3000	20820		4.3		82														40	2.5			
3-6-47	1500	20850	.25	2.0	175	3.5	475	340	473	469	383	463	455	464	374	443	233	124	289	.0018	1.4	40.5	GAGE PRESS 11.5 PSI	SP 8-3-78
		20820		4.3		82														36	2.6			





Figures 7 through 10 show test bearing and oil outlet temperatures as a function of the inner-ring-path oil flow for Lube/Cooling flow ratios of 1/4.0, 1/3.0, 1/1.33 and 1/0.

Referring to Figure 7 for the  $L_1/C_1 = 1/4.0$  ratio, the inner ring temperatures varied from 252°C to 272°C (485°F to 522°F) depending upon the inner ring lube path flow ( $C_1 + L_1$ ).

The outer ring temperatures ranged generally from 260°C (500°F) to 288°C (550°F) and were, as expected, affected by both the oil flow to the inner ring and the amount of cooling oil supplied to this component.

The oil outlet temperatures generally paralleled the inner ring temperatures from 243°C (470°F) to 264°C (507°F). Neither the inner race nor the oil outlet temperatures were significantly influenced by the outer ring cooling oil flow.

Figures 8, 9 and 10 show corresponding results for the other inner ring flow ratios tested.

The results of the 1/3.0 flow ratio were similar, but the temperatures of the inner race were slightly higher. Outer ring temperatures are generally lower at the low inner ring path flow rates and slightly higher at the higher flow rates.

Bearing temperatures in excess of 288°C (550°F) at low flow rates and drive power limitations of the test machine at high flow rates limited the number of tests with 1/1.33 and 1/0.0 lube flow ratios. For those tests which were successfully completed, the resulting temperatures were somewhat higher.

In Figures 11 through 14, bearing temperatures are plotted as functions of the  $C_1/L_1$  ratio for oil flows to the inner rings of 126 (2.0), 189 (3.0), 221 (3.5) and 252 (4.0) cm<sup>3</sup>/sec (gpm), respectively. Flow ratios resulting in minimum outer ring temperatures were discovered for an inner ring path flow of 189 cm<sup>3</sup>/sec (3.0 gpm). Inner ring and oil out temperatures decreased with increasing flow ratios. It is interesting to note that, for total flow rates ( $C_1 + L_1$ ) of 189 (3.0) and 221 cm<sup>3</sup>/sec (3.5 gpm), practical flow ratios were found for balanced bearing temperature operation. From the curves for 126 (2.0) and 252 cm<sup>3</sup>/sec (4.0 gpm) total flow, ratios may be extrapolated to find potential conditions for balanced bearing operation.

The small number of points on Figures 13 and 14 limit the conclusions that can be drawn from this data.

Power as a function of oil flow to the inner rings is shown in Figures 15 through 18. As would be expected, the power demand increases markedly with increasing inner ring path flow, but is not affected by outer ring cooling oil flow. The power demand for the entire system ranged from 66 to 91 kilowatts. If a 98% efficiency of the belt drive and a 2 kilowatt power demand by the support bearing are assumed, the range of power per bearing was on the order of 31 to 44 kilowatts.

ORIGINAL PAGE IS  
OF POOR QUALITY

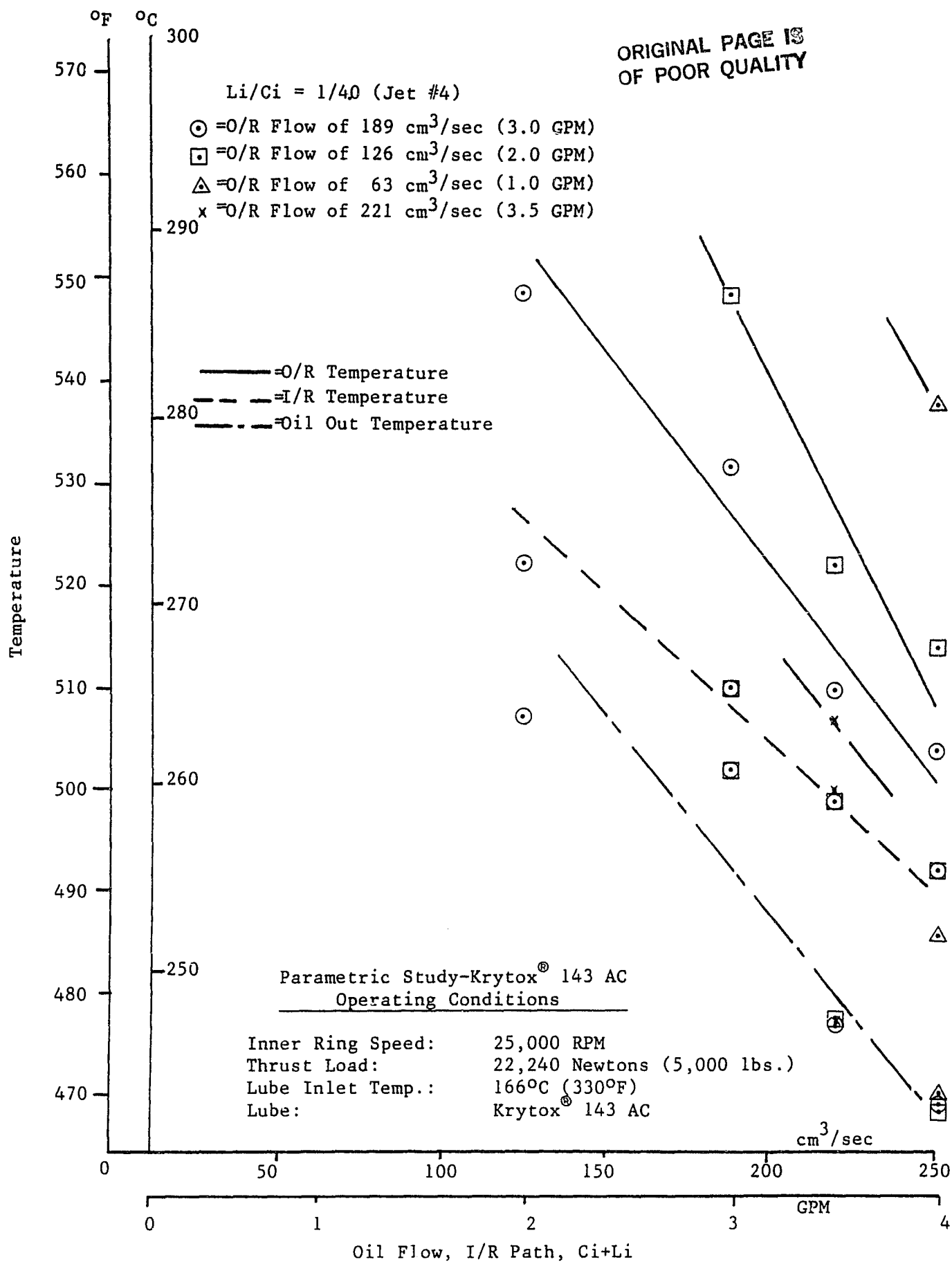


Figure 7. Bearing Temperatures vs. Inner Ring Path Oil Flow and Lube-to-Cooling Flow Ratios of 1/4.0.

ORIGINAL PAGE IS  
OF POOR QUALITY

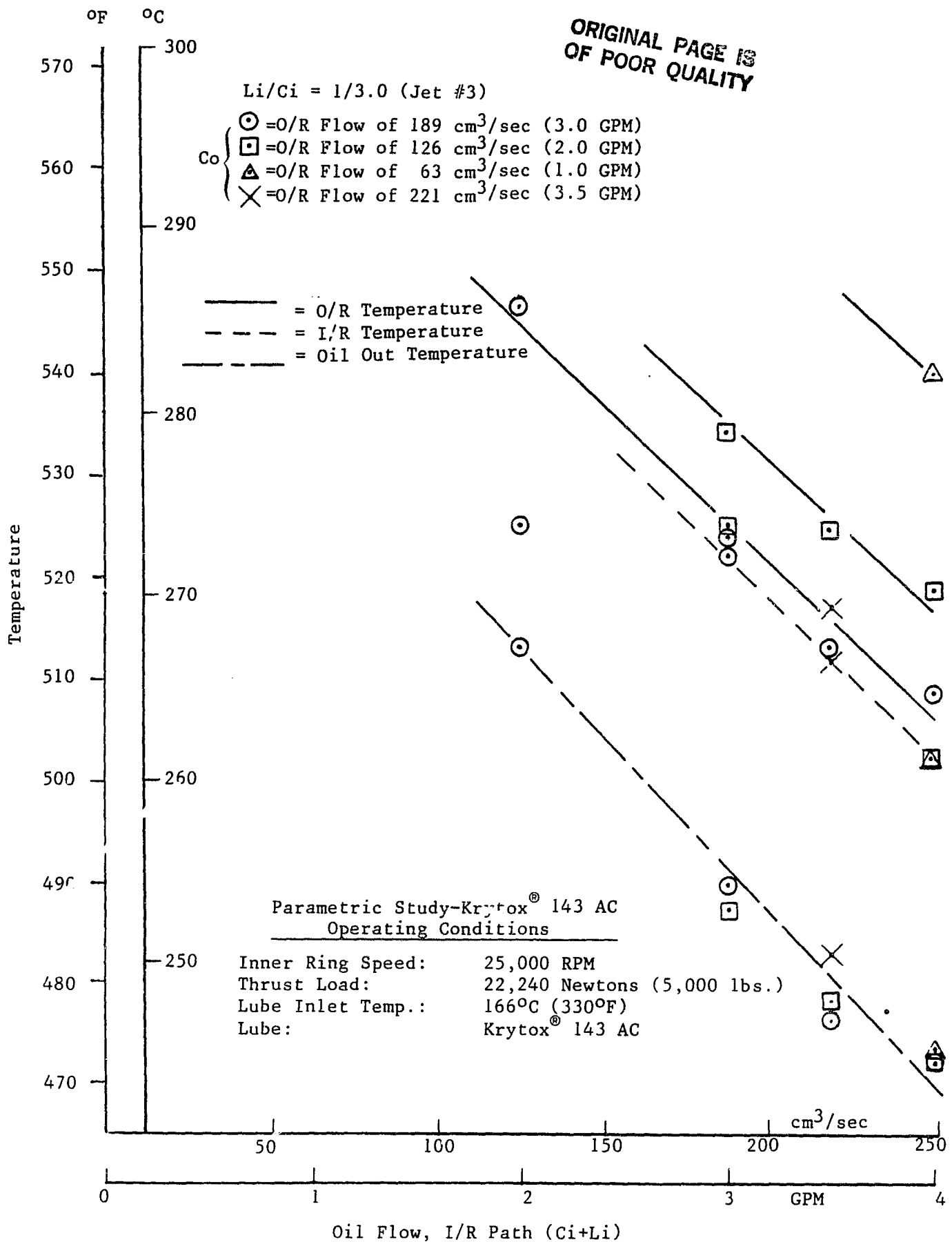


Figure 8. Bearing Temperatures vs. Inner Ring Path Oil Flow for Lube-to-Cooling Flow Ratios of 1/3.0.

ORIGINAL PAGE IS  
OF POOR QUALITY

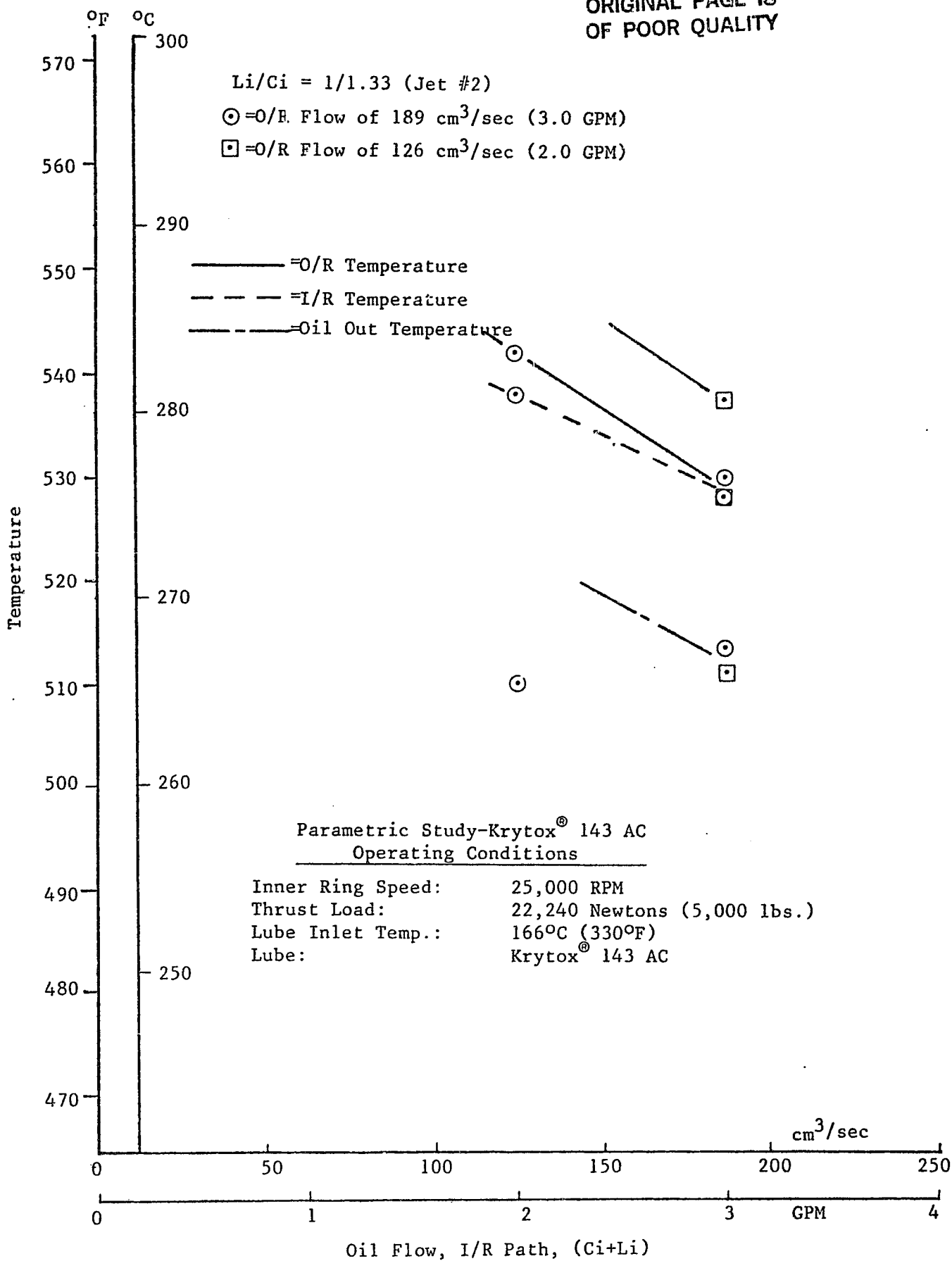


Figure 9. Bearing Temperatures vs. Inner Ring Path Oil Flow for Lube-to-Cooling Flow Ratios of 1/1.33.

ORIGINAL PAGE IS  
OF POOR QUALITY

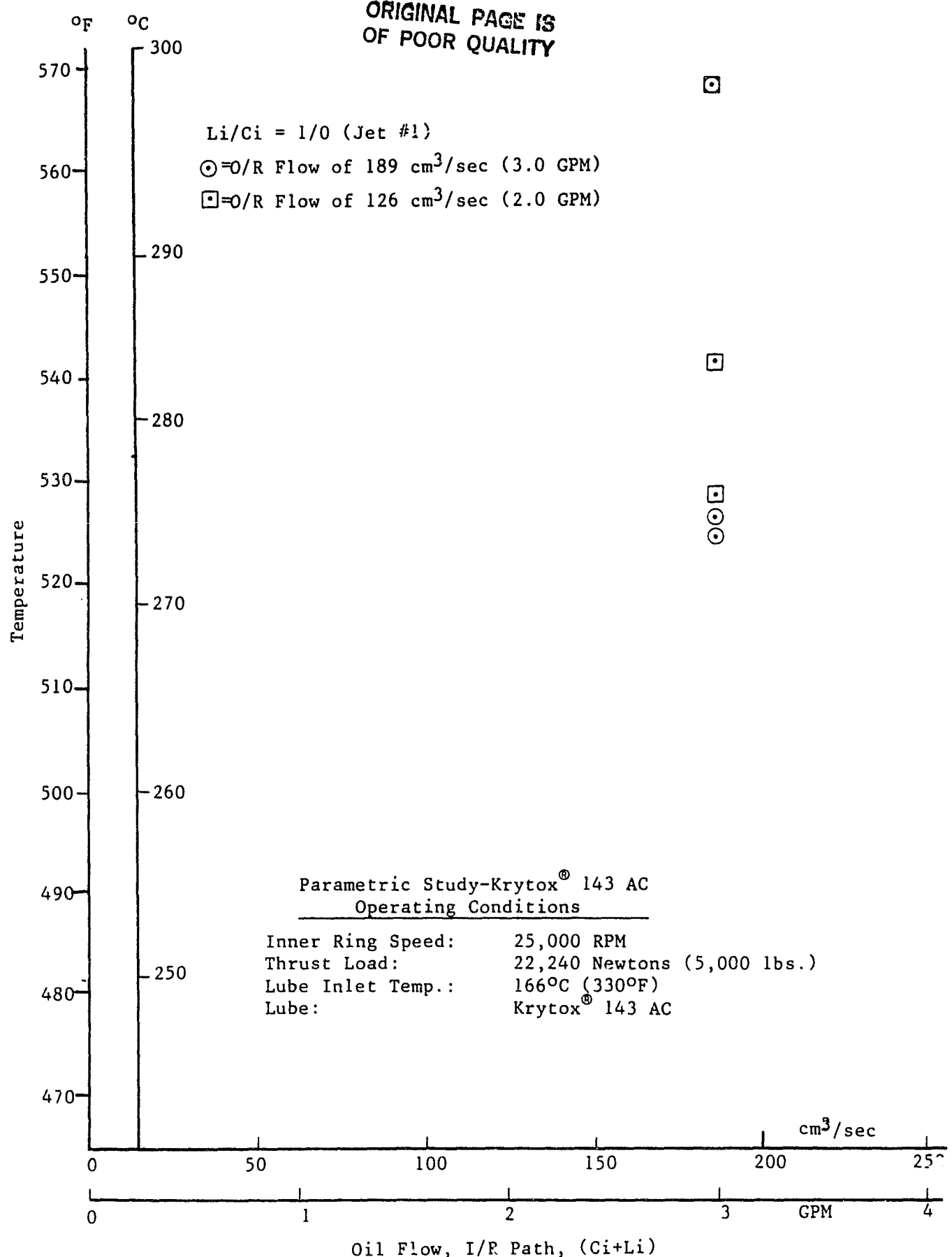


Figure 10. Bearing Temperatures vs. Inner Ring Path Oil Flow for Lube-to-Cooling Flow Ratios of 1/0.

ORIGINAL PAGE IS  
OF POOR QUALITY

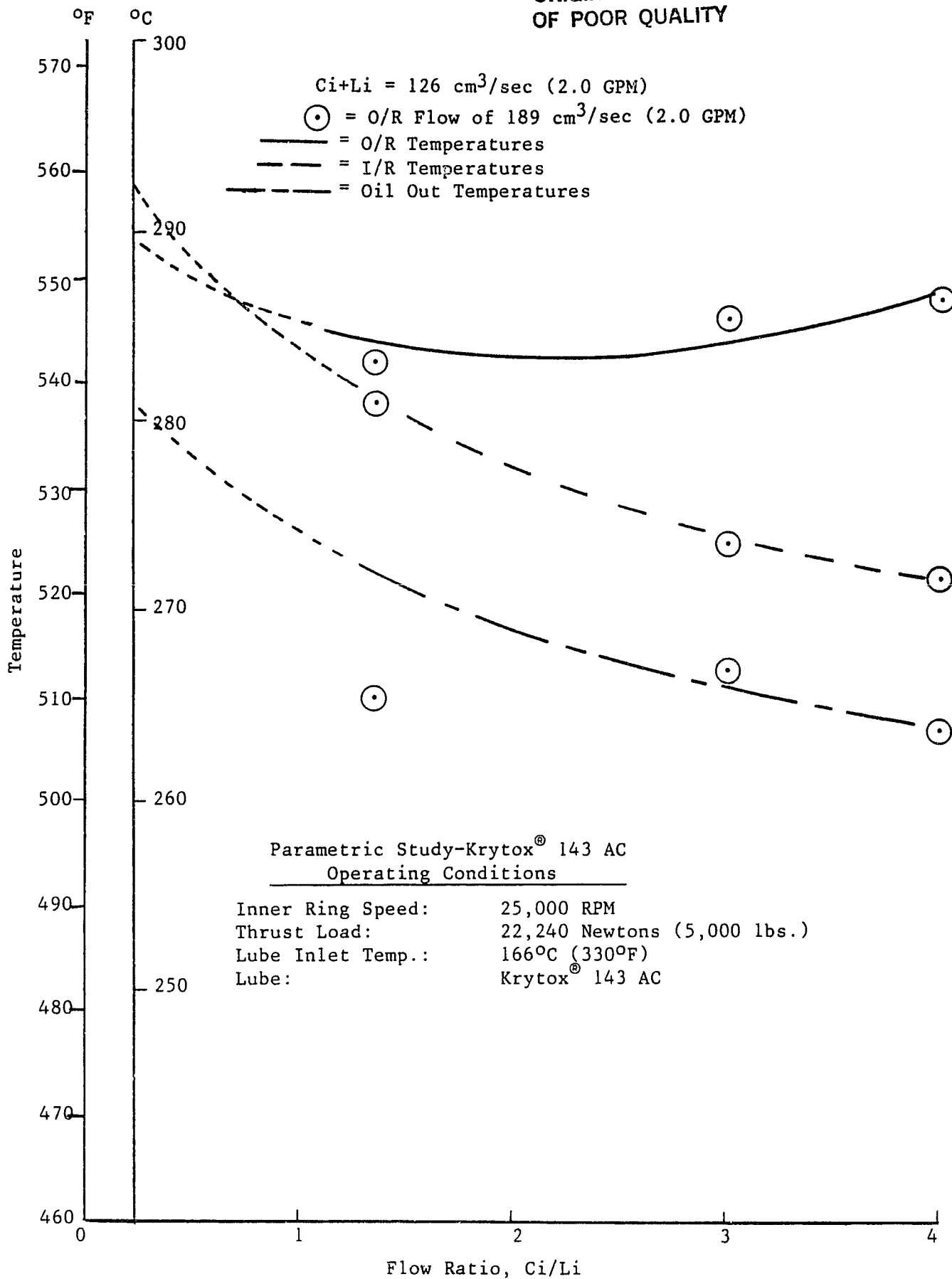


Figure 11. Bearing Temperatures vs. Inner Ring Path Coolant-to-Lube Ratios at a Total Coolant plus Lube Flow Rate of  $126 \text{ cm}^3/\text{sec}$ .

ORIGINAL PAGE IS  
OF POOR QUALITY

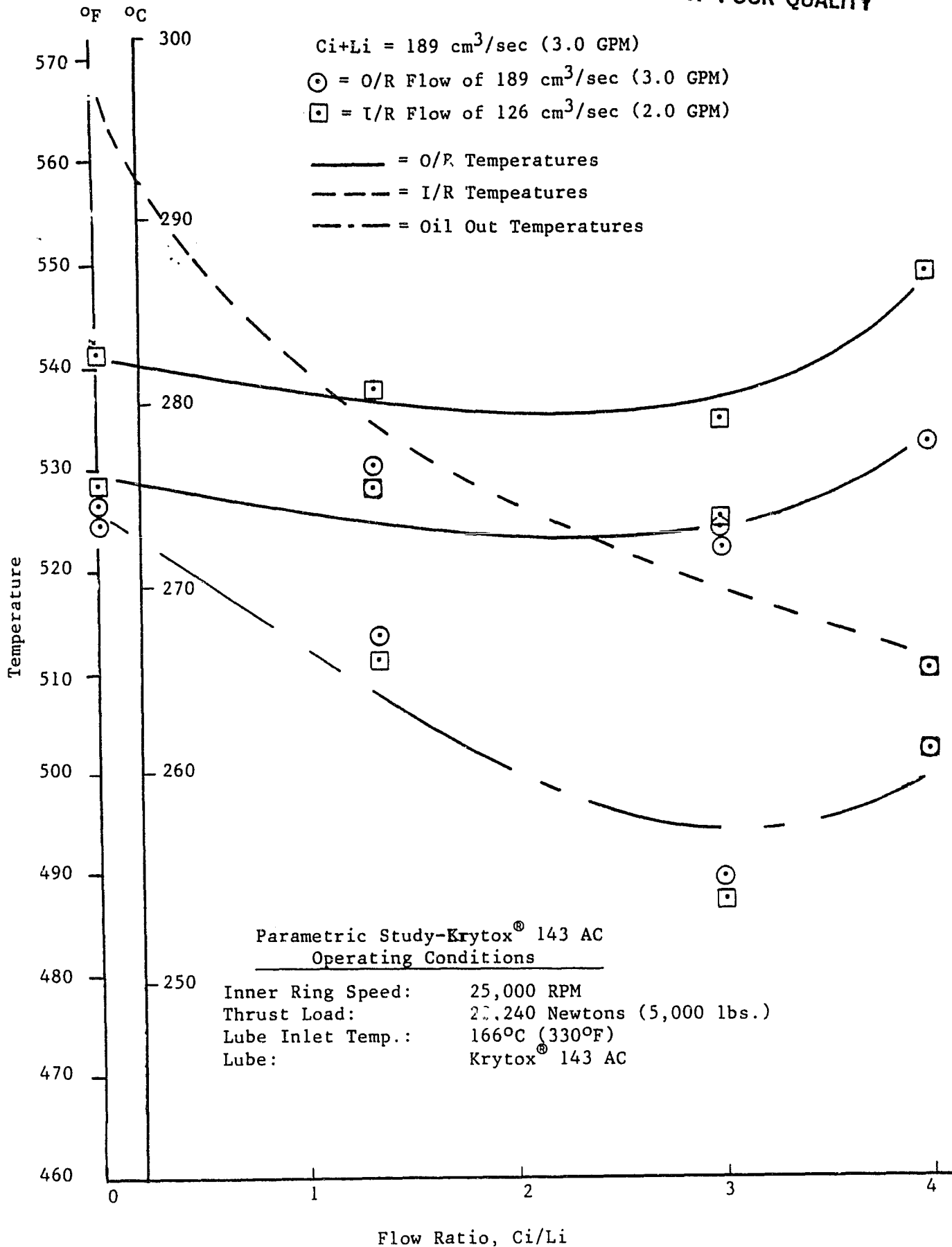


Figure 12. Bearing Temperatures vs. Inner Ring Path Coolant-to-Lube Ratios at a Total Coolant plus Lube Flow Rate of  $189 \text{ cm}^3/\text{sec}$ .

ORIGINAL PAGE IS  
OF POOR QUALITY

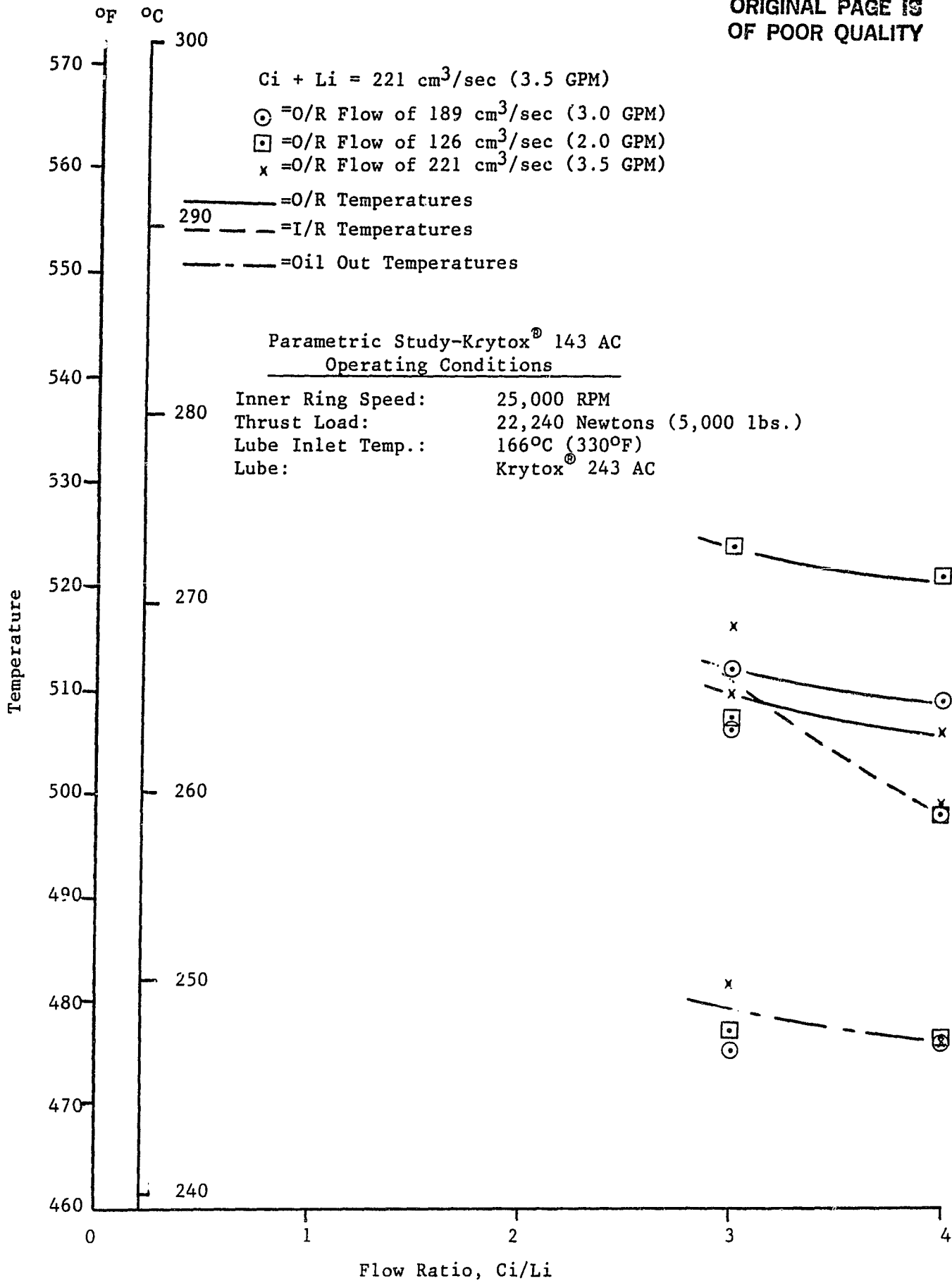


Figure 13. Bearing Temperatures vs. Inner Ring Path Coolant-to-Lube Ratios at a Total Coolant plus Lube Flow Rate of  $221 \text{ cm}^3/\text{sec}$ .

ORIGINAL PAGE IS  
OF POOR QUALITY

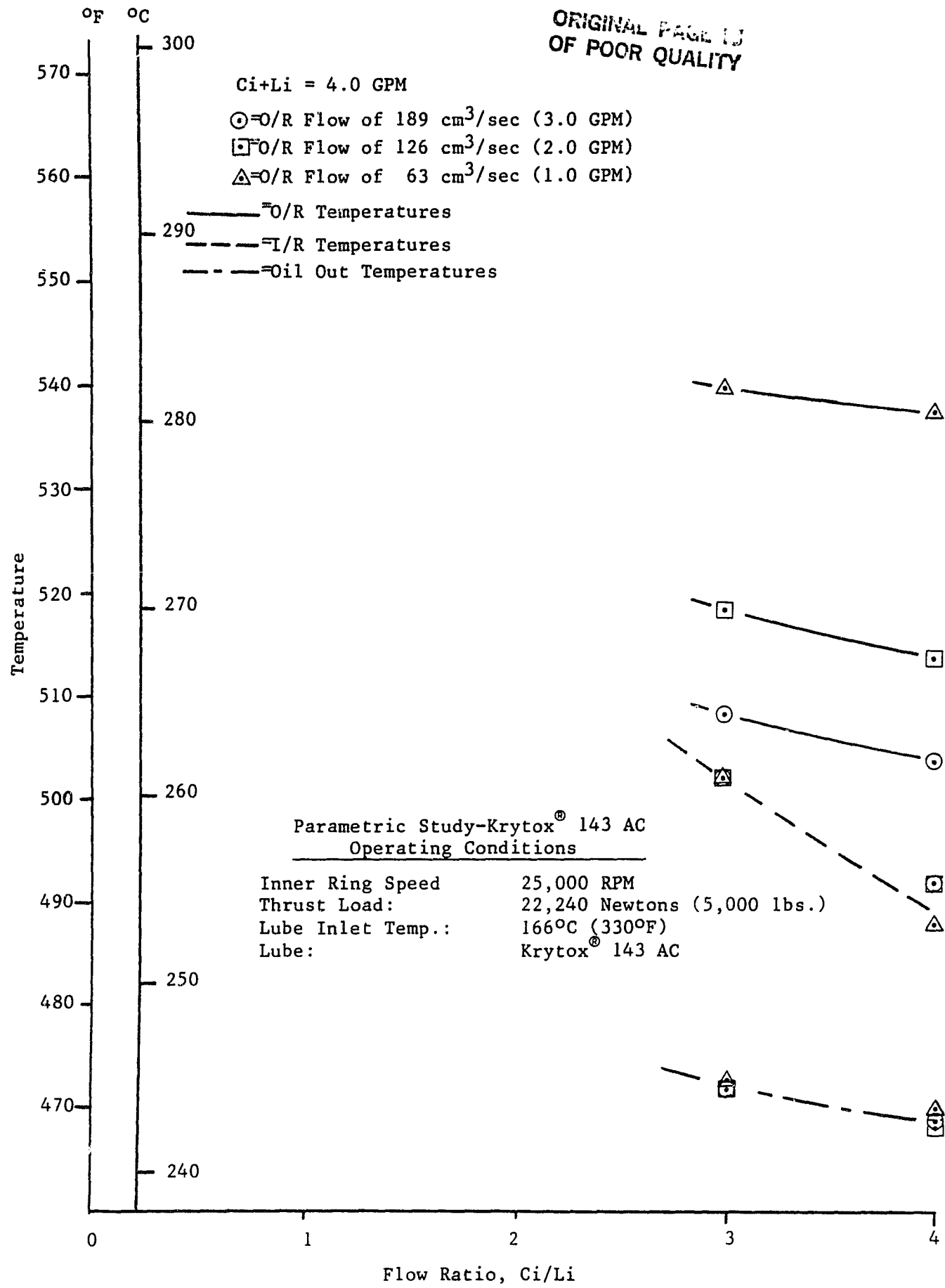


Figure 14. Bearing Temperatures vs. Inner Ring Path Coolant-to-Lube Ratios at a Total Coolant plus Lube Flow Rate of 252 cm<sup>3</sup>/sec.

ORIGINAL PAGE IS  
OF POOR QUALITY

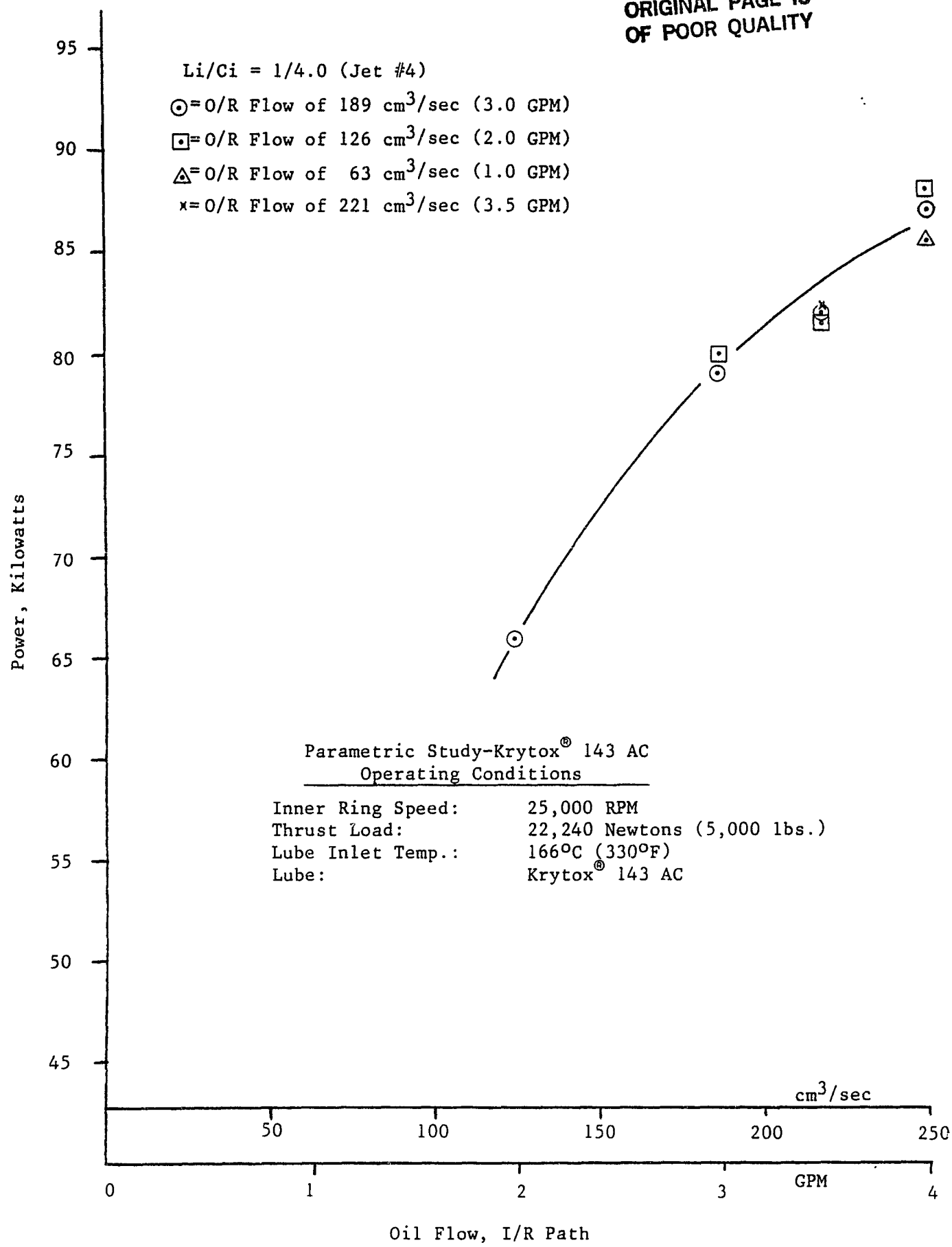


Figure 15. Bearing Power vs. Inner Ring Path Oil Flow at a Lube-to-Coolant Flow Ratio of 1/4.0.

ORIGINAL PAGE IS  
OF POOR QUALITY

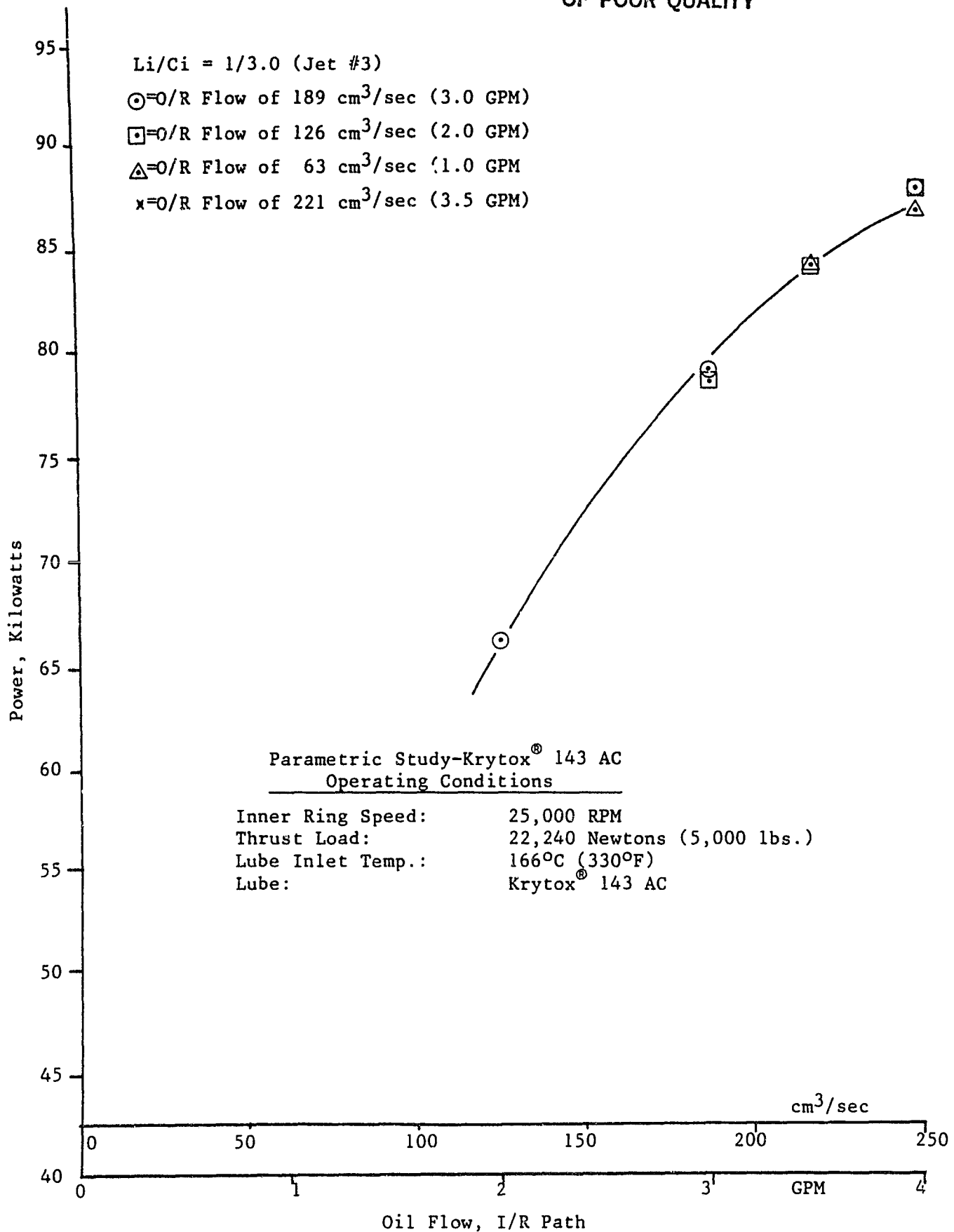


Figure 16. Bearing Power vs. Inner Ring Path Oil Flow at a Lube-to-Coolant Flow Ratio of 1/3.0.

ORIGINAL PAGE IS  
OF POOR QUALITY

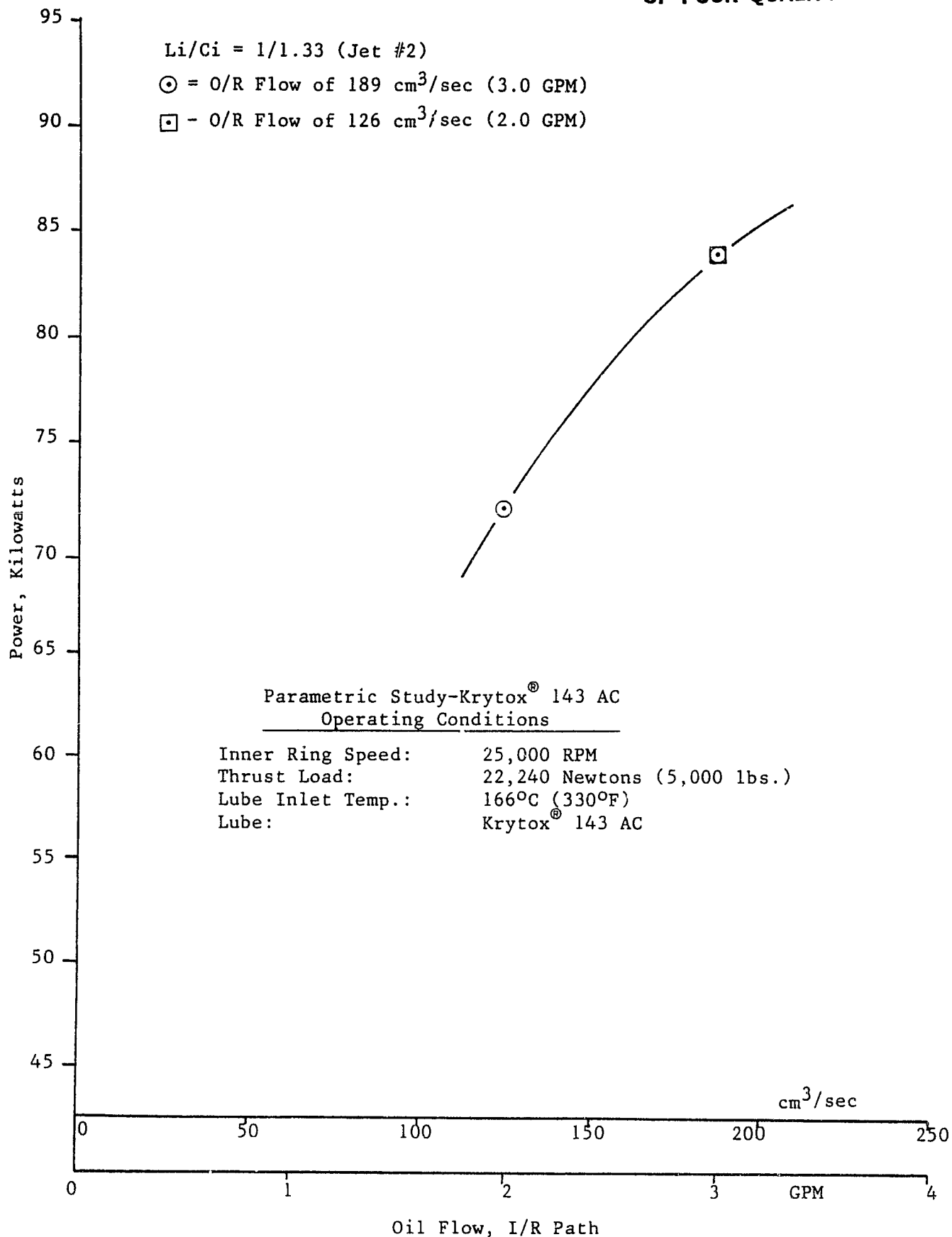


Figure 17. Bearing Power vs. Inner Ring Path Oil Flow at a Lube-to-Coolant Flow Ratio of 1/1.33.

ORIGINAL PAGE IS  
OF POOR QUALITY

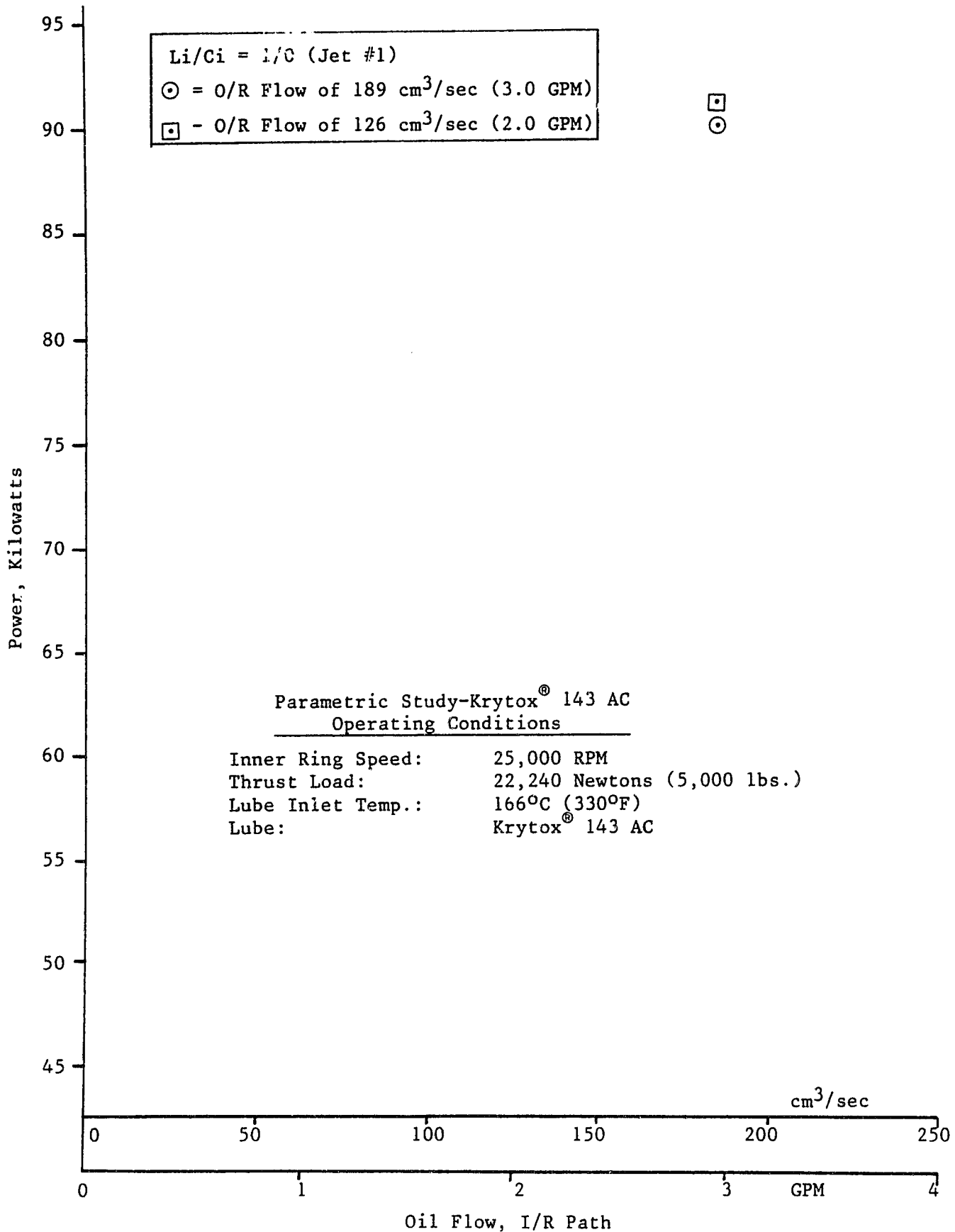


Figure 18. Bearing Power vs. Inner Ring Path Oil Flow at a Lube-to-Coolant Flow Ratio of 1/0.

As seen in Figures 15 and 16, the power demand curves for flow ratios of 1/4.0 and 1/3.0 are virtually identical. Though fewer data points are available, the power required for  $L_i/C_i$  ratios of 1/1.33 and 1/0.0 is significantly higher.

The power data was replotted in Figures 19 through 22 as functions of inner ring flow ratio,  $C_i/L_i$ . A minimum power loss is suggested for total flows ( $C_i + L_i$ ) of 126 (2.0) and 189  $\text{cm}^3/\text{sec}$  (3.0 gpm) at a flow ratio  $C_i/L_i$  of about 3.0.

### 3.3.2 Bearing Life Evaluation

The test bearings were from the same manufacturing lot and material heat as those of the previous endurance test program described (9). With these bearings, lives of 3,000 hours were achieved repeatedly using a type II oil. In an earlier test program reported in (1,4 and 5), 120 mm ball bearings of CEVM\*M50 were tested at 1.4 million DN and  $316^\circ\text{C}$  ( $600^\circ\text{F}$ ) in a nitrogen atmosphere using Krytox 143 AC as a lubricant. In that program, typical bearing lives on the order of 100 to 500 hours were achieved.

After an initial 10 hours of testing to the original planned test conditions, i.e., ring temperatures of  $316^\circ\text{C}$  ( $600^\circ\text{F}$ ), signs of bearing failures were noticed. On both test bearings, the inner and outer races were severely pitted at the load tracks. The outer race of the front bearing showed severe corrosion or erosion pitting on either side of the load track. Signs of corrosive attack and surface distress were also evident on the balls, and the separators showed heavy ball pocket wear and moderate wear at the lands.

These observations made it clear that, similar to the parametric study, high speed operation with ring temperatures at  $316^\circ\text{C}$  ( $600^\circ\text{F}$ ) would not be feasible with an open, non-inerted system. The life test conditions were, therefore, also modified for a maximum bearing temperature of  $288^\circ\text{C}$  ( $550^\circ\text{F}$ ).

Lowering the operating temperature reduced the severity of corrosion damage on the test bearings during subsequent tests. However, very short bearing life, typically on the order of 5 to 15 hours, were still encountered throughout the remainder of this program. A tabulation of bearing life is given in Table VI. The Weibull analysis on these data is as follows:

B-10 Life:	4.02 hours
B-50 Life:	10.61 hours
Slope:	1.94
Failure Index:	17/17

As mentioned earlier in a previous investigation (1), rolling-element fatigue tests were conducted with 120 mm bore angular-contact ball bearings of AISI M50 steel with the same Krytox fluid. Here at  $316^\circ\text{C}$  ( $600^\circ\text{F}$ ) under a low-oxygen environment, the Krytox gave bearing lives approximately 3 times AFBMA.\*\* Bearing failure was predominantly subsurface initiated, although some corrosion pitting was observed. However, corrosion was not considered to be the primary cause for spalling failure.

\* Consumable Electrode Vacuum Melted

\*\* Anti-Friction Bearing Manufacturers' Association

ORIGINAL PALE IS  
OF POOR QUALITY

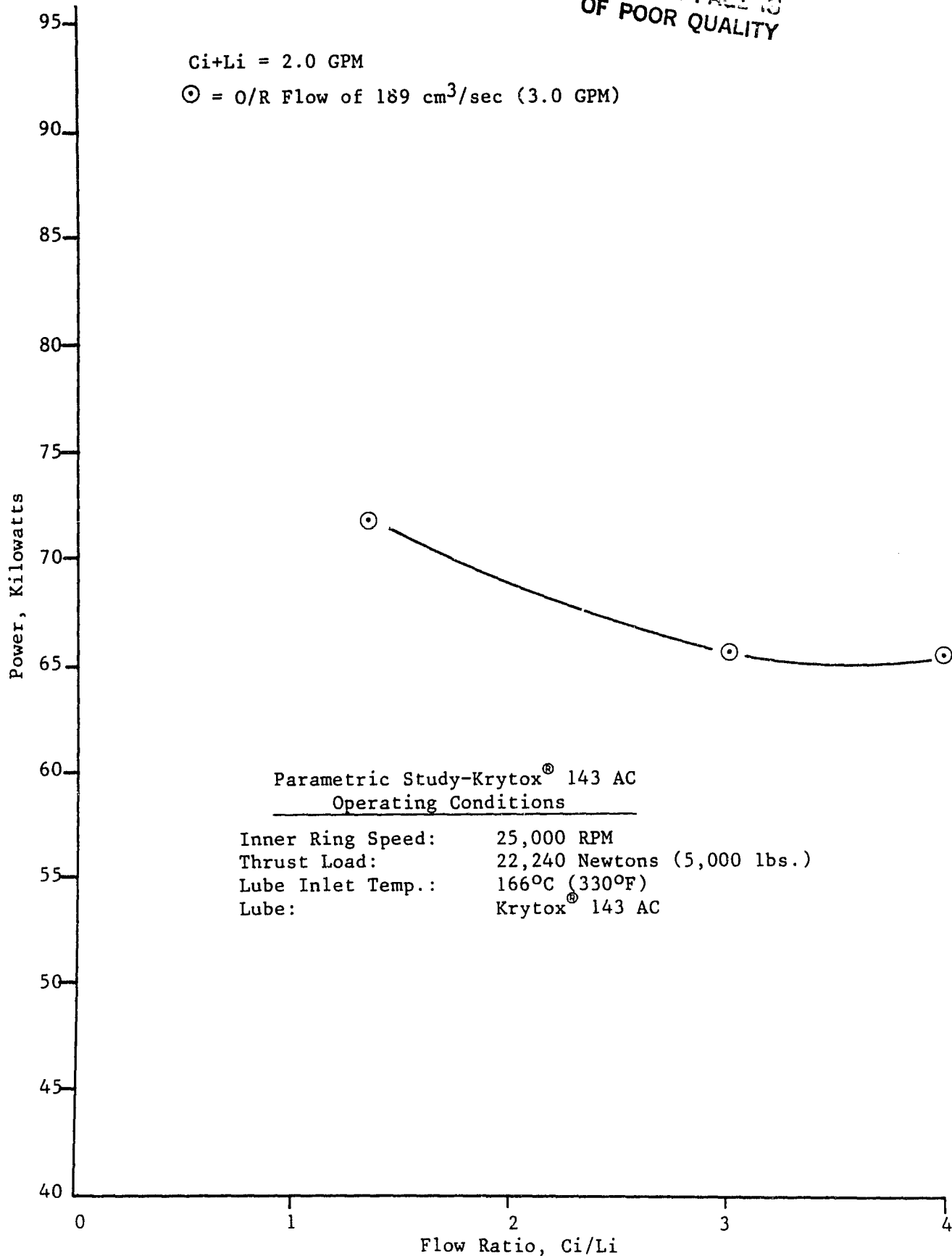


Figure 19. Bearing Power vs. Inner Ring Flow Path Coolant-to-Lubricant Flow Ratios for a Total Coolant plus Lube Flow Rate of 126 cm<sup>3</sup>/sec.

ORIGINAL PAGE IS  
OF POOR QUALITY

$C_i+L_i = 189 \text{ cm}^3/\text{sec}$  (3.0 GPM)

⊙ = O/R Flow of  $189 \text{ cm}^3/\text{sec}$  (3.0 GPM)

□ = O/R Flow of  $126 \text{ cm}^3/\text{sec}$  (2.0 GPM)

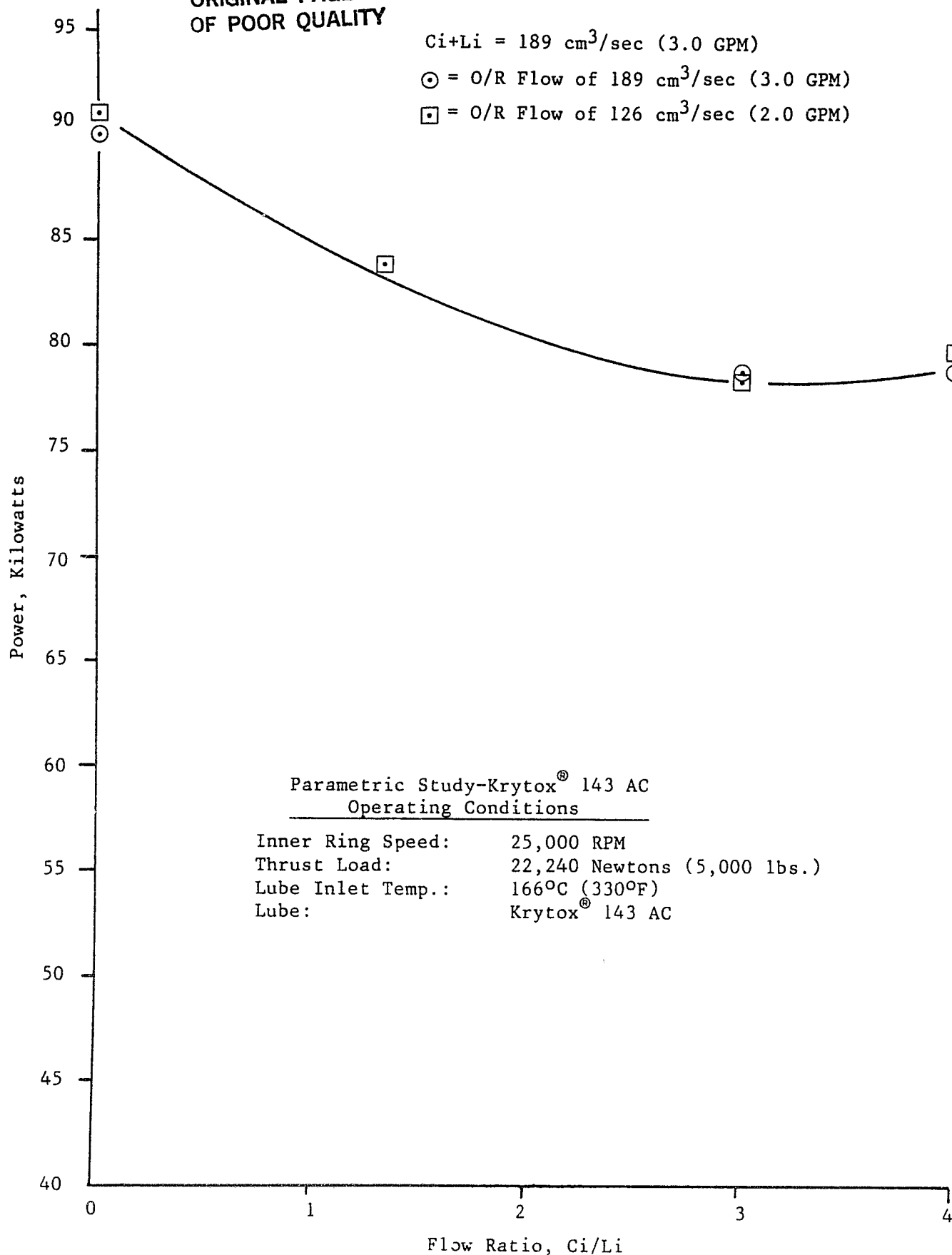


Figure 20. Bearing Power vs. Inner Ring Flow Path Coolant-to-Lubricant Flow Ratios for a Total Coolant plus Lube Flow Rate of  $189 \text{ cm}^3/\text{sec}$ .

ORIGINAL PAGE IS  
OF POOR QUALITY

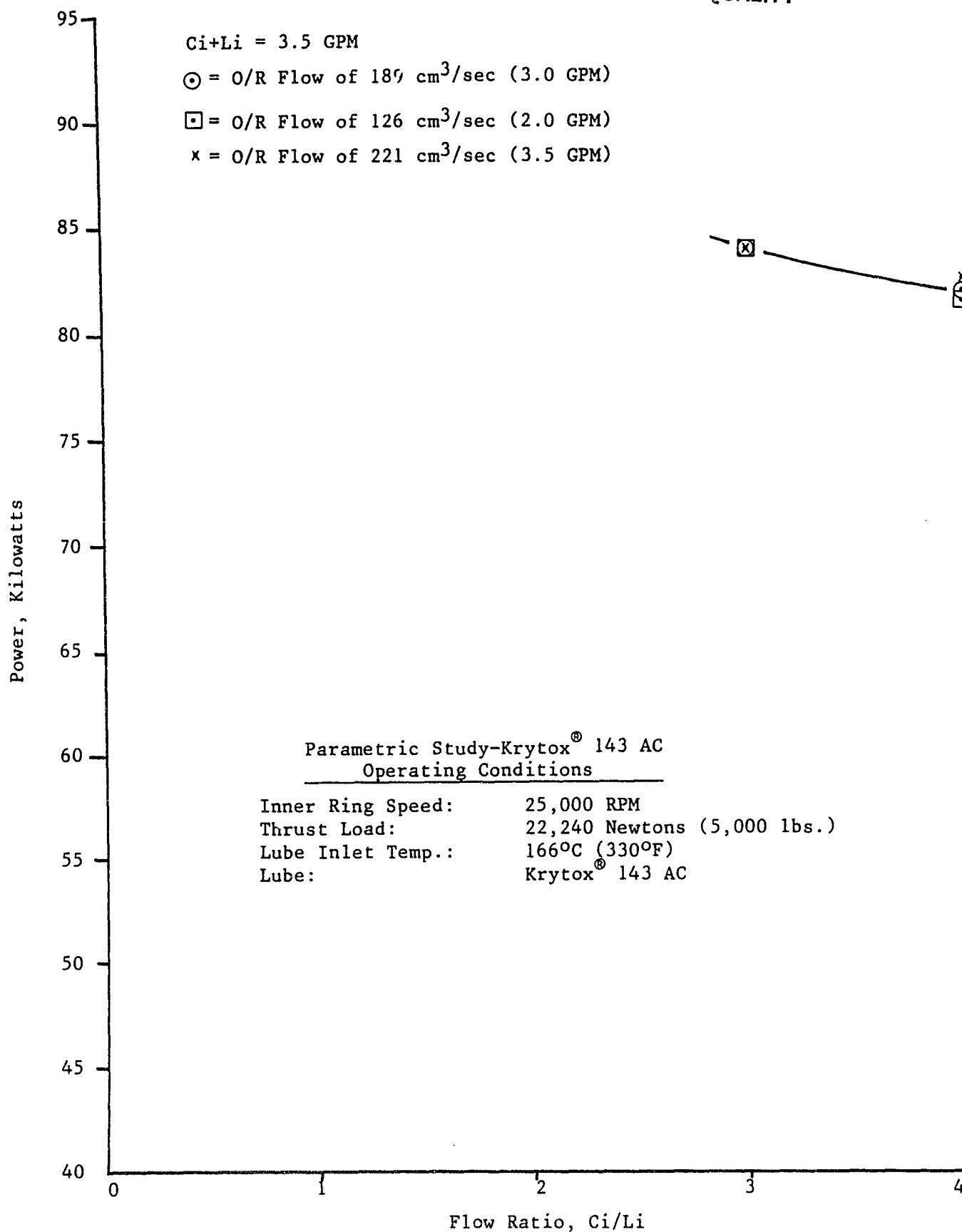


Figure 21. Bearing Power vs. Inner Ring Flow Path Coolant-to-Lubricant Flow Ratios for a Total Coolant plus Lube Flow Rate of 221 cm<sup>3</sup>/sec.

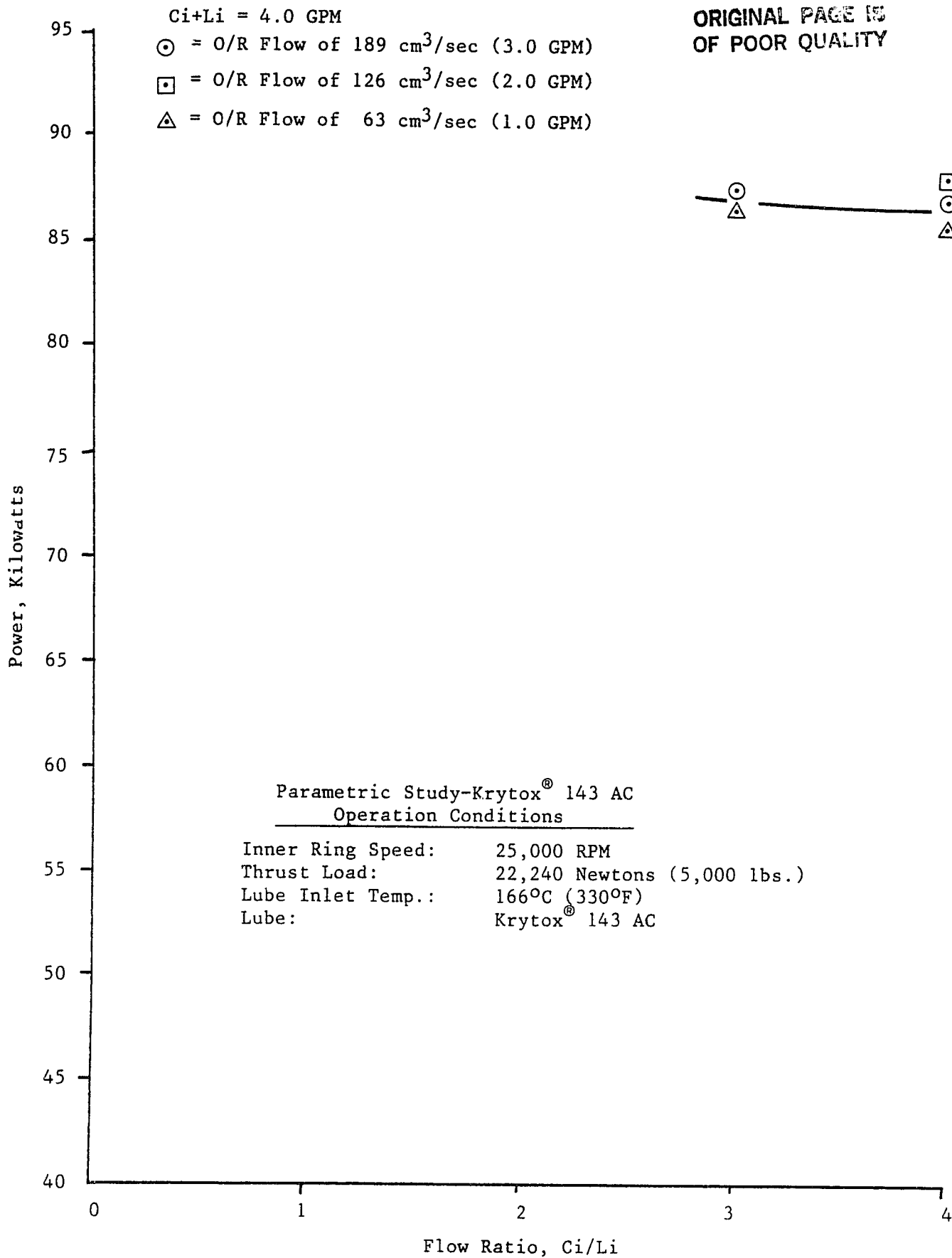


Figure 22. Bearing Power vs. Inner Ring Flow Path Coolant-to-Lubricant Flow Ratios for a Total Coolant plus Lube Flow Rate of 252 cm<sup>3</sup>/sec.

TABLE VI

Summary of Bearing Tests, Test Life and Post-Test Condition

Brg. S/N	Test No.	Position	Test Hrs.	Loading	Brg. Condition After Test
100	II-1	F	17	"T" O/R S/N 1/R	Light Corrosion/Pitting on Raceways. Balls OK
	I-7	F	14	S/N O/R "T" 1/R	New Balls. Raceways Corroded. Balls OK
116	II-1	R	17	"T" O/R S/N 1/R	Slight Corrosion on Raceways. Balls OK
	I-7	R	14	S/N O/R "T" 1/R	O/R Corroded. Fatigue Spalls on 1/R and Balls
105	I-2	F	15	"T" O/R S/N 1/R	Raceways Corroded Balls Fair Shape
	I-8	F	3	S/N O/R "T" 1/R	O/R Corroded. 1/R OK Balls Have Surface Distress.
109	I-8	R	3	"T" O/R S/N 1/R	Light Corrosion and a Few Debris Dents. Balls OK
110	I-6	F	13	"T" O/R S/N 1/R	Corrosion on Raceways. 1 Ball Has Small Debris Dent.
66	I-2	R	15	"T" O/R S/N 1/R	Raceways Corroded. One Ball Has Fatigue Spall.
	I-3	R	5	S/N O/R "T" 1/R	Possible Inclusion in O/R. One Ball with Fatigue Spall.
108	I-3	F	5	"T" O/R S/N 1/R	Numerous Debris Dents in Raceway.
	I-4	R	15	S/N O/R "T" 1/R	3 Balls Have Pitting - Replaced for I-5.
	I-5	R	10	S/N O/R S/N 1/R	Raceways Corroded and Pitted. Spalls on Balls.
120	I-6	R	13	"T" O/R S/N 1/R	Raceways Corroded. Balls Have Spalling.

ORIGINAL PAGE IS  
OF POOR QUALITY

TABLE VI (CONT'D.)

Summary of Bearing Tests, Test Life and Post-Test Condition

Brg. S/N	Test No.	Position	Test Hrs.	Loading	Brg. Condition After Test
118	I-4	F	15	"T" O/R S/N 1/R	Severe Raceway Corrosion All Balls Have Spalling
	I-5	F	10	S/N O/R "T" 1/R	Raceways Mildly Corroded. Balls OK
56	I-1	F	10	"T" O/R S/N 1/R	Severe Pitting/Corrosion on Raceways. Surface Distress/Corrosion on Balls.
71	I-1	R	10	"T" O/R S/N 1/R	Pitting/Corrosion on Raceways and Balls.

Figures 23 through 28 are provided to illustrate typical bearing failure characteristics encountered in the most recent tests, operating with the Krytox 143 fluid in air. Raceway failures were limited to surface pitting (micro-spalling). Examples of these are shown in Figures 23, 24 and 26. Ball failures were more severe. These failures, which had the appearance of classical sub-surface fatigue spalling, were associated with little or no evidence of surface distress. Figure 28 shows this. Figure 27 shows the wear on the ball pockets.

During one of the disassemblies to replace a failed bearing, a dark deposit was noted on one of the machine surfaces. Samples of the deposit as well as samples of the lubricant in the test machine were subjected to fluorescent X-ray analyses. A sample of unused Krytox was also analyzed for comparison.

The results of the particulate analyses indicated substantial amount of iron, nickel and chrome. The analyses of the new and used lubricant showed essentially identical compositions. From this, it was concluded that no major decomposition of the lubricant, per se, had taken place. The deposits were wear particles from the rolling contact surfaces of the balls and races and the separator plating.

### 3.3.3 Data Reliability and Ball Passing Frequency

Throughout this test program, difficulties were experienced in collecting consistent bearing performance data. Repeated runs of the same test often produced different temperatures, particularly when the tests occurred near the extremes of the test conditions. Therefore, the test results reported are a selection of data that was the most consistent and reliable of those measured. There still remain, however, some temperature points that do not fit well with the rest of the data. Typical examples are shown in Figures 9 through 11 (for  $C_1/L_1 = 1.33$ ;  $(C_1 + L_1) = 126 \text{ cm}^3/\text{sec}$  (2.0 gpm)). Here the "lube-out" temperature appears to be on the order of  $6^\circ\text{C}$  ( $10^\circ\text{F}$ ) below where it might be expected, based on the results of adjacent tests. A close examination of the data will indicate several such anomalies.

It may be speculated that some data inconsistency was caused by varying levels of ball slippage. This appears possible with the use of the high density Krytox lubricant, which caused the deterioration of raceway finish with increasing test time.

In an attempt to confirm this theory, an effort was made to determine the ball passing frequency. The signal from an accelerometer on the test housing was applied to a spectrum analyzer and the spectrum was recorded in the range of the anticipated ball passing frequency. A typical spectrum is shown in Figure 29. Unfortunately, there are at least two signals in the anticipated frequency range, either of which could represent the ball passing frequency. One of the signals is quite near the anticipated frequency as reported in (8), while the other is somewhat lower. Frequency measurements at different lube flow rates did not fall within the expected pattern, making definitive identifications difficult.

ORIGINAL PAGE IS  
OF POOR QUALITY



Figure 23. Inner Race Failure in Bearing S/N 116.

ORIGINAL PAGE IS  
OF POOR QUALITY



Figure 24. Inner Race Failure in Bearing S/N 116.

ORIGINAL PAGE IS  
OF POOR QUALITY



Figure 25. Overall View of Bearing S/N 118.

ORIGINAL PAGE IS  
OF POOR QUALITY

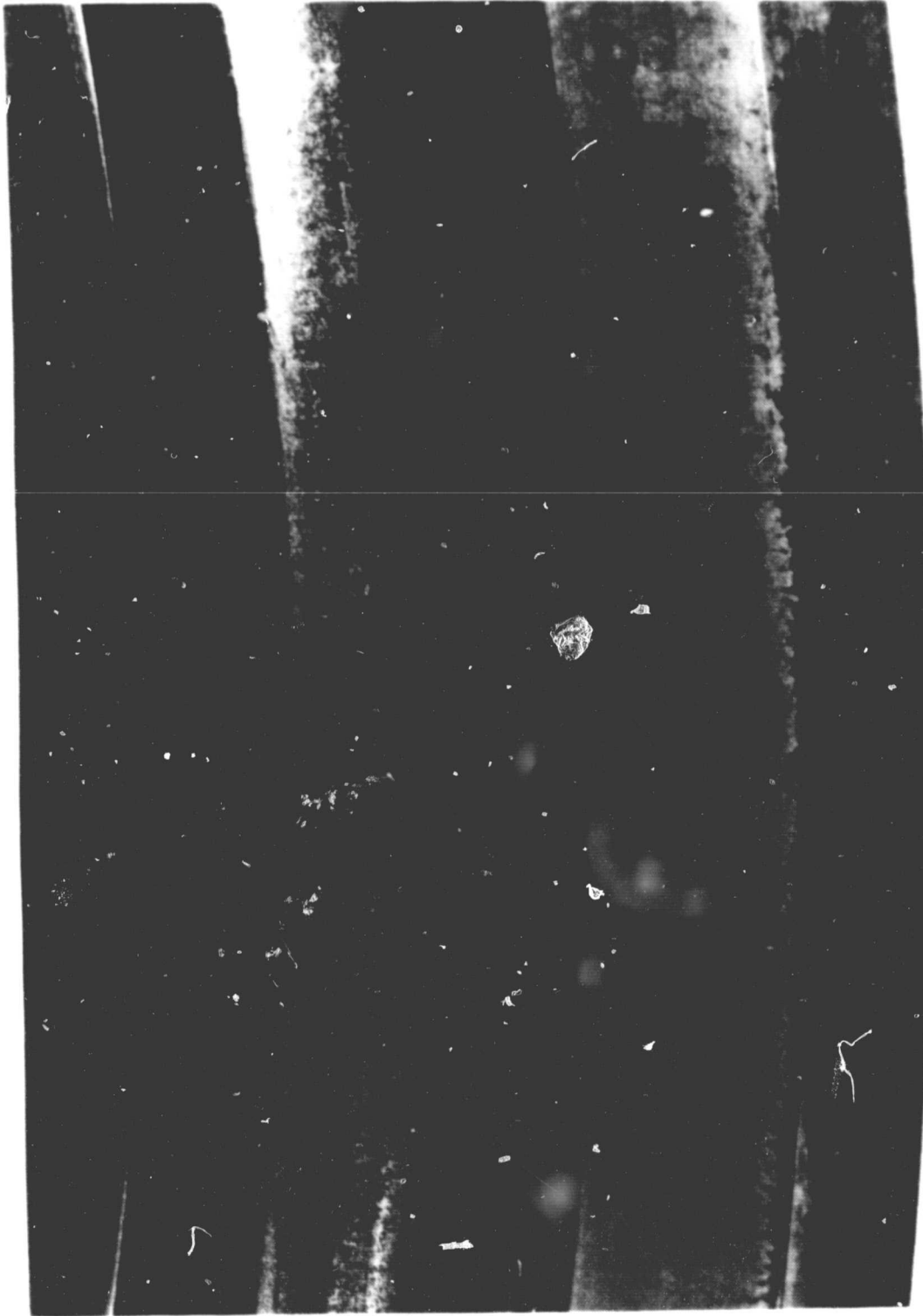


Figure 26. Outer Race Failure in Bearing S/N 118.

ORIGINAL PAGE IS  
OF POOR QUALITY

Typical Wear  
in Ball Pockets

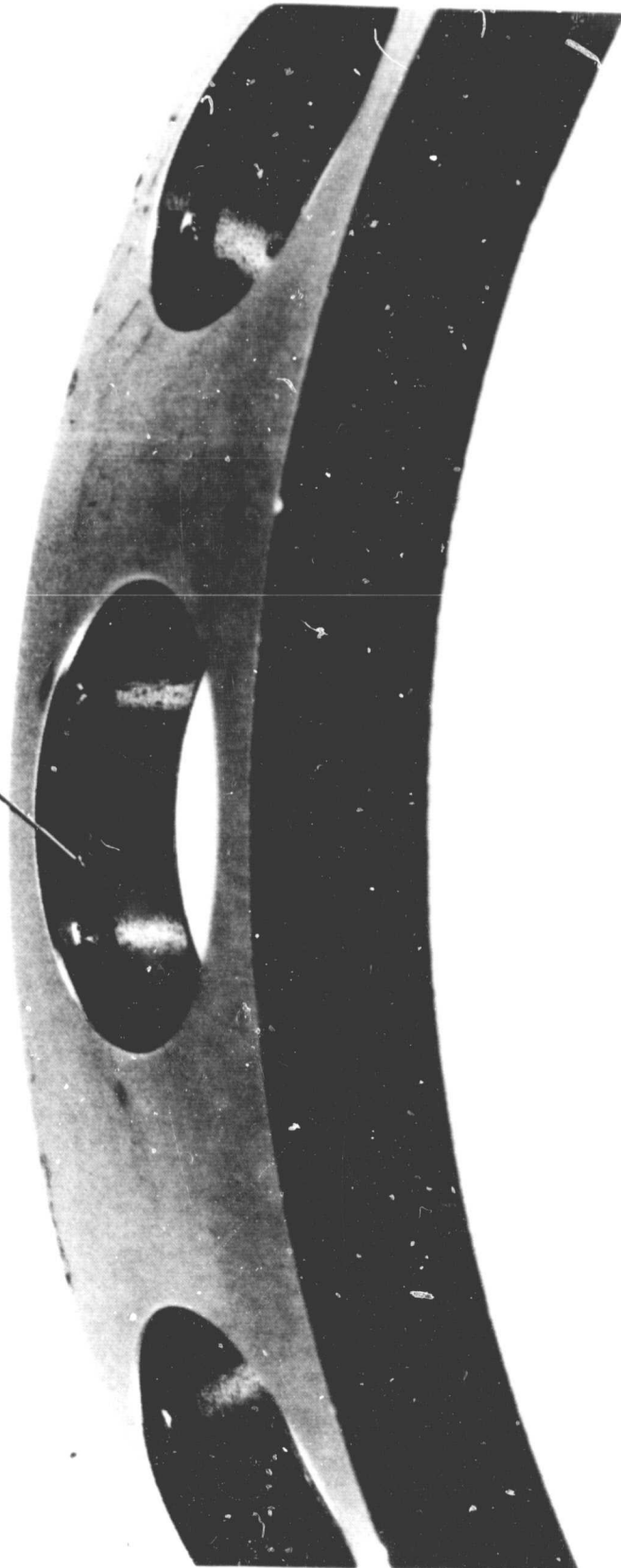


Figure 27. Cage for Bearing S/N 118.

ORIGINAL PAGE IS  
OF POOR QUALITY

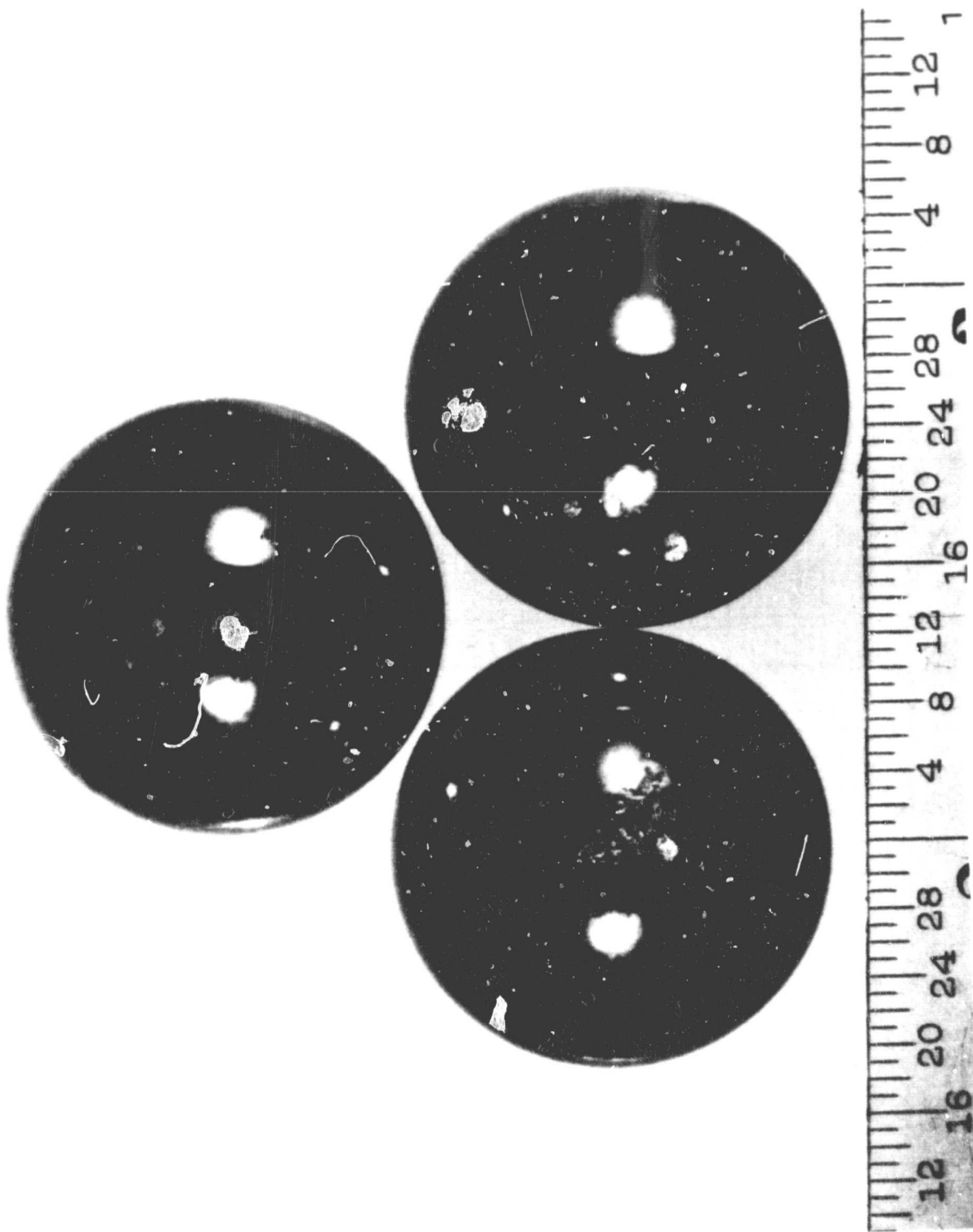


Figure 28. Balls from Bearing S/N 118.

ORIGINAL PAGE IS  
OF POOR QUALITY

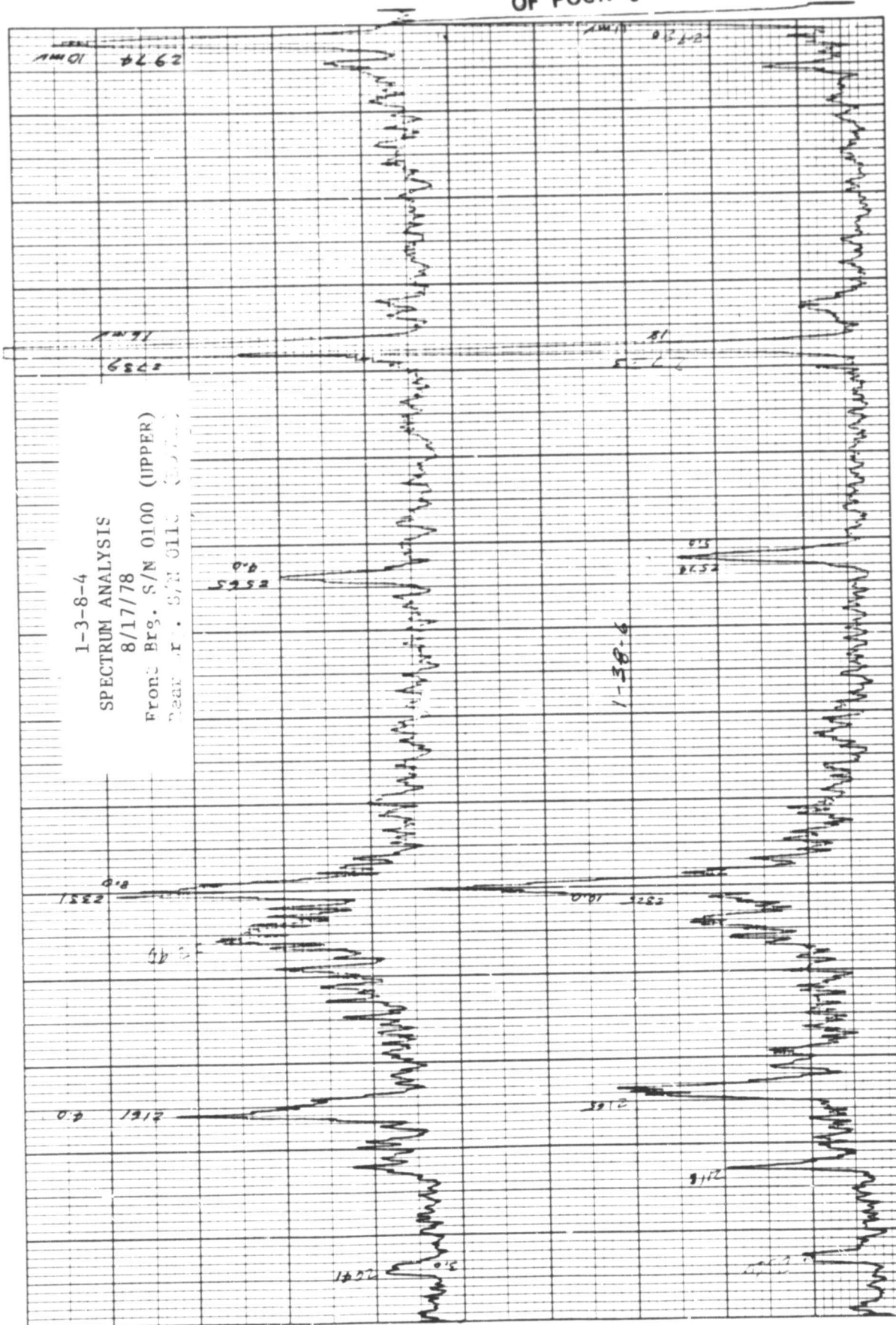


Figure 29. Ball Passing Acceleration - Frequency Spectrum for Bearings S/N 100 and 116.

### 3.3.4 Additional Parametric Studies - Effect of Speed and Load

A lubricant flow ratio and an inner ring oil flow were chosen from those initial test results which produced the most favorable bearing performance at 25,000 rpm with a thrust load of 22,240 Newtons (5,000 lbs.). The lubricant inlet temperature and outer ring cooling oil flow were further adjusted until a thermally balanced bearing operating condition was achieved, such that the inner and outer bearing rings were maintained at 288°C (550°F). The values that produced this condition, within a 1.7°C (3°F) spread, were held constant throughout this test phase. Those values were:

$L_i/C_i$	-	1/3.0
Lube flow, inner ring path	-	126 cm <sup>3</sup> /sec (2.0 gpm)
Cooling oil flow, outer ring path	-	221 cm <sup>3</sup> /sec (3.5 gpm)
Lube inlet temperature	-	171°C (340°F)

The effects of loads and inner ring speeds were investigated, and the results are presented in Table V and in Figures 30 through 34.

Bearing temperatures as a function of load are shown in Figure 30. Bearing outer ring temperature increased nearly linearly with load for a particular speed; i.e., the temperature rise over the load range was greater for high speed operation than for low speed. For example, the outer ring temperature increased only 2.2°C (4°F) due to increasing the load from 1,500 to 5,000 lbs. at 12,000 rpm. The same load increase at 25,000 rpm resulted in a 18°C (33°F) temperature rise. The effect on the inner ring temperature was somewhat more dramatic. Contrary to expectations, at 12,000 rpm the temperature dropped as the load was increased. At 16,700 rpm, the temperature remained constant throughout the load range, and at 25,000 rpm, the inner and outer ring temperatures increased nearly at the same rate with increasing loads. In Figures 31 and 32, the bearing temperature data were re-plotted as a function of inner ring speed.

The machine power demand is shown as a function of load and of speed in Figures 33 and 34, respectively. These curves illustrate the expected trends of modest power increase due to increasing load and a sharp rise in the power demand for increasing speeds.

### 3.4 TASK III CONCLUSIONS

Parametric tests were conducted with 120 mm bore, angular contact, split-inner-ring, AISI M50 ball bearings. A polymeric perfluorinated fluid, marketed by DuPont under the trade name Krytox 143 AC, was used as the lubricant in an air atmosphere. The following conclusive remarks can be made:

1. Practical limits were experienced for the range of lubricant flow to the test bearings. Low flow rates produced bearing temperatures beyond the upper, acceptable limit. High flow rates increased the power demand beyond the capacity of the test rig drive motor.

ORIGINAL PAGE IS  
OF POOR QUALITY

--- = I/R Temperature  
— = O/R Temperature

⊙ = 25,000 RPM  
□ = 20,850 RPM  
△ = 16,700 RPM  
x = 12,000 RPM

Operating Conditions for Phase II

Flow Ratio:  $L_i/C_i = 1/3.0$   
 Oil Flow, I/R Path:  $126 \text{ cm}^3/\text{sec}$  (2.0 GPM)  
 Oil Flow, O/R Path:  $221 \text{ cm}^3/\text{sec}$  (3.5 GPM)  
 Lube Inlet Temp.:  $172^\circ\text{C}$  ( $340^\circ\text{F}$ )  
 Lube: Krytox<sup>®</sup> 143 Ae

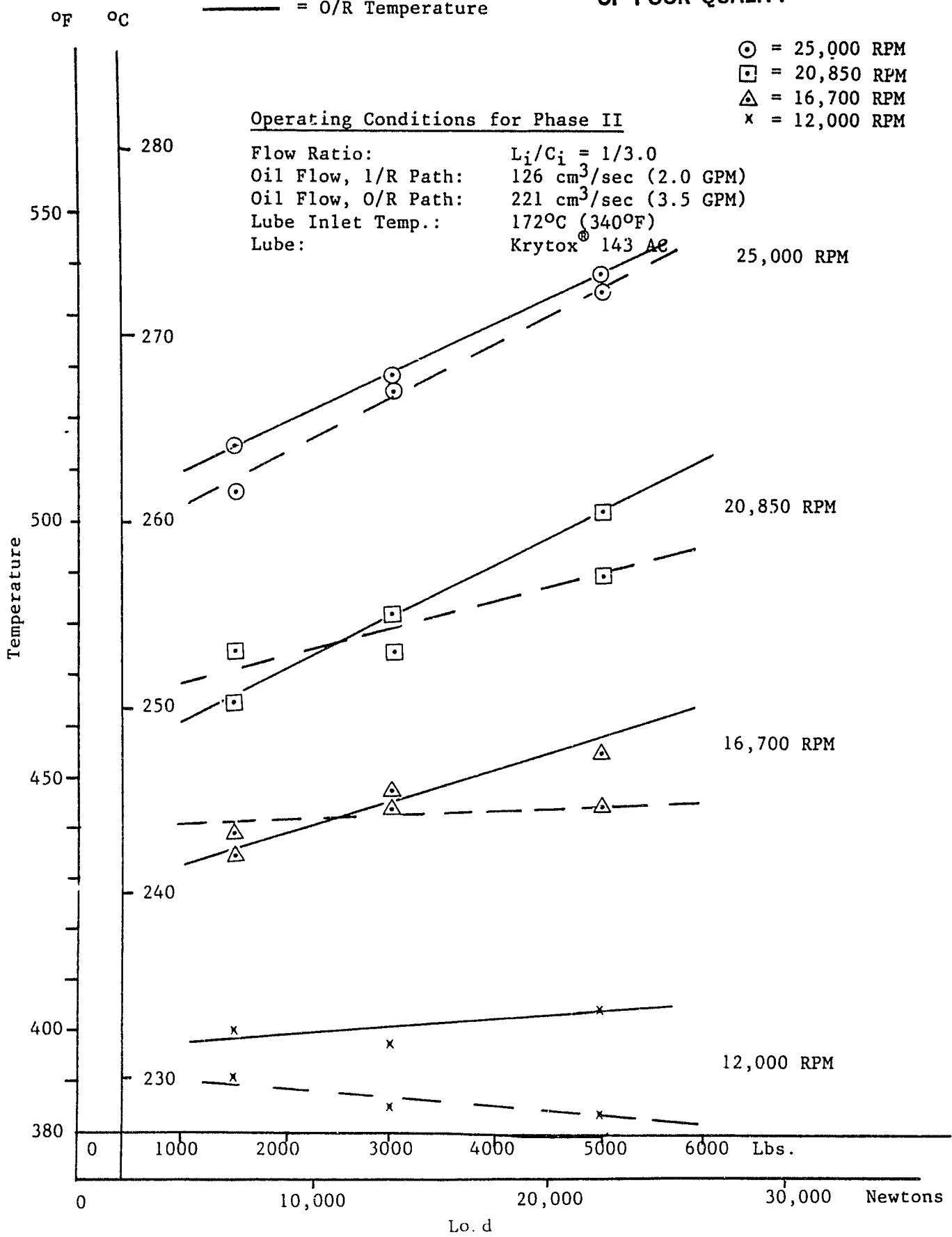


Figure 30. Bearing Temperature vs. Load at Various Speeds.

ORIGINAL PAGE IS  
OF POOR QUALITY

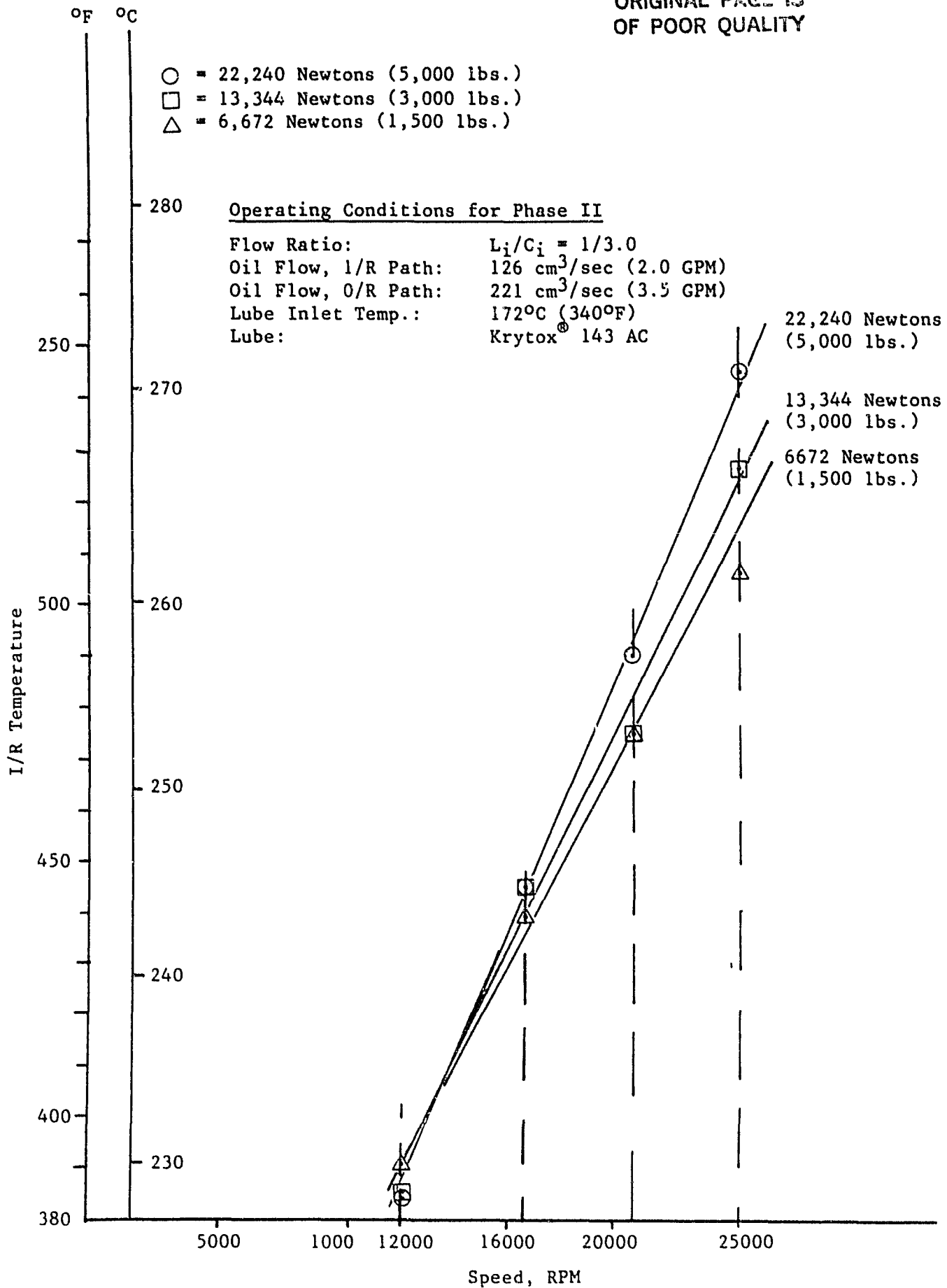


Figure 31. Inner Race Temperature vs. Speed at Various Loads.

ORIGINAL PAGE IS  
OF POOR QUALITY

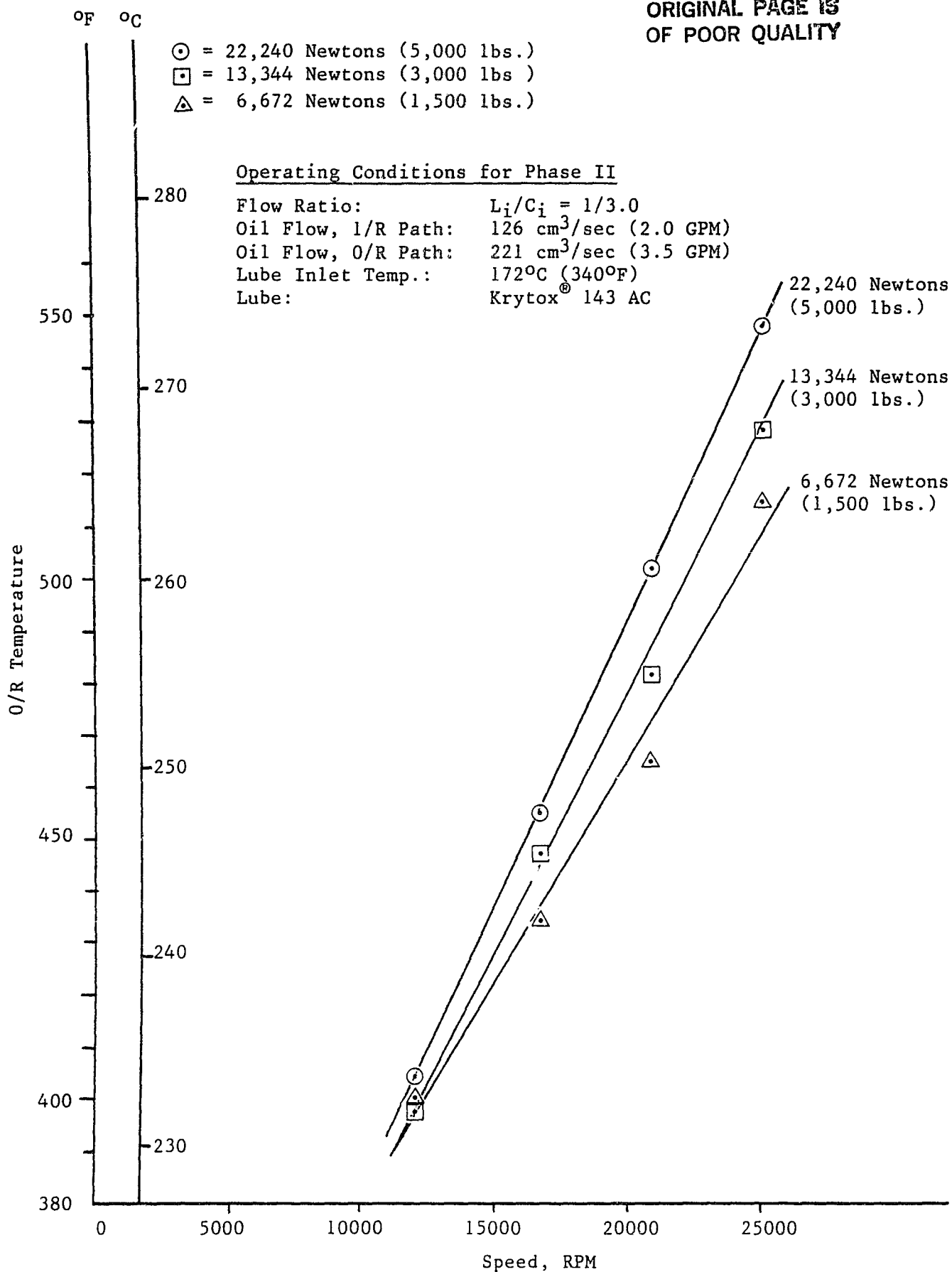


Figure 32. Outer Race Temperature vs. Speed at Various Loads.

- ⊙ = 25,000 RPM
- ◻ = 20,850 RPM
- △ = 16,700 RPM
- x = 12,000 RPM

ORIGINAL PAGE IS  
OF POOR QUALITY

Operating Conditions for Phase II

Flow Ratio:  $L_i/C_i = 1/3.0$   
 Oil Flow, 1/R Path:  $126 \text{ cm}^3/\text{sec}$  (2.0 GPM)  
 Oil Flow, 0/R Path:  $221 \text{ cm}^3/\text{sec}$  (3.5 GPM)  
 Lube Inlet Temp.:  $172^\circ\text{C}$  ( $340^\circ\text{C}$ )  
 Lube: Krytox® 143 AC

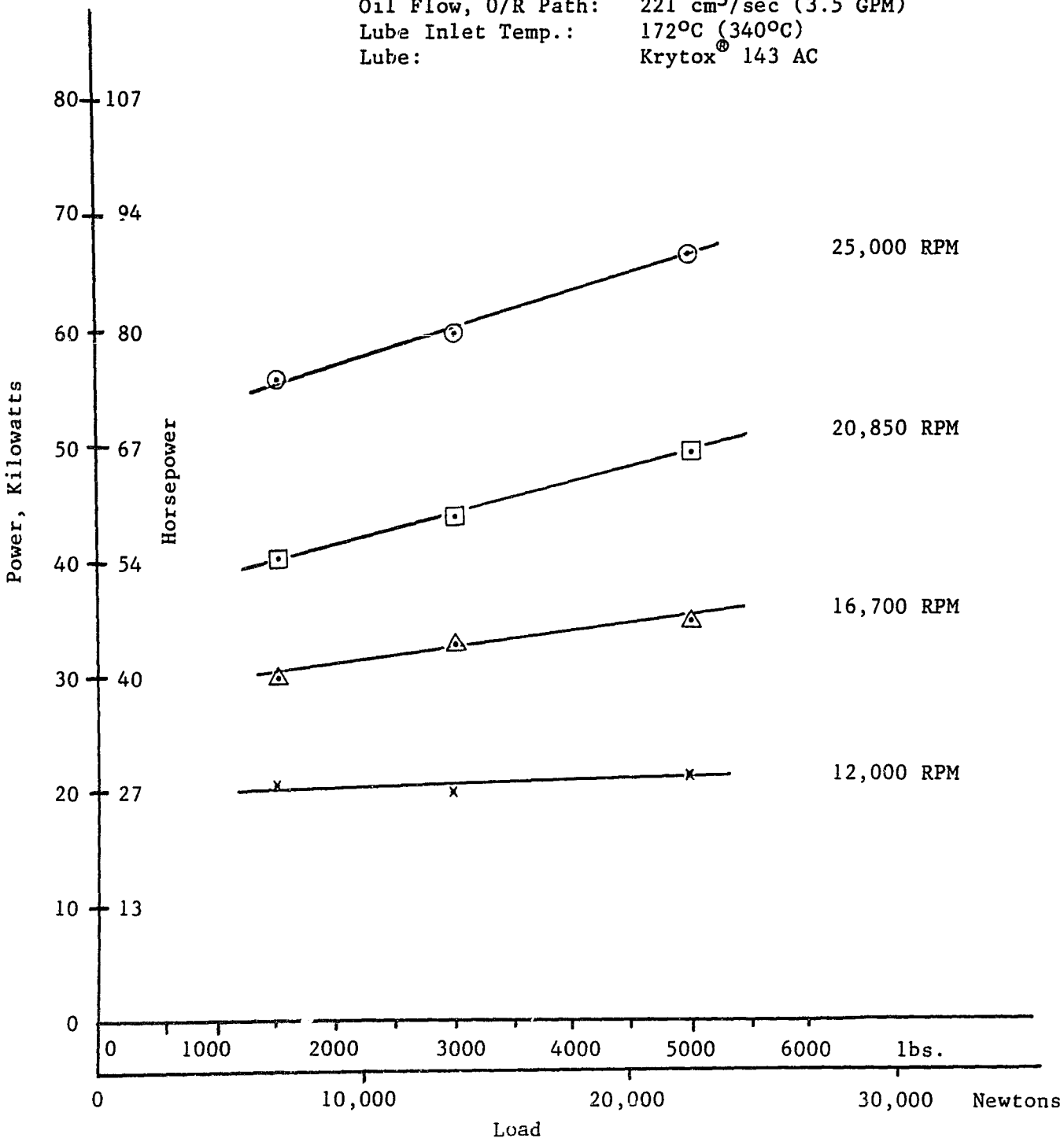


Figure 33. Bearing Power vs. Load at Various Speeds.

ORIGINAL PAGE IS  
OF POOR QUALITY

- ⊙ = 22,240 Newtons (5,000 lbs.)
- ◻ = 13,344 Newtons (3,000 lbs.)
- △ = 6,672 Newtons (1,500 lbs.)

Operating Conditions For Phase II

Flow Ratio:  $L_i/C_i = 1/3.0$   
Oil Flow, 1/R Path:  $126 \text{ cm}^3/\text{sec}$  (2.0 GPM)  
Oil Flow, O/R Path:  $221 \text{ cm}^3/\text{sec}$  (3.5 GPM)  
Lube Inlet Temp.:  $172^\circ\text{C}$  ( $340^\circ\text{F}$ )  
Lube: Krytox<sup>®</sup> 143 AC

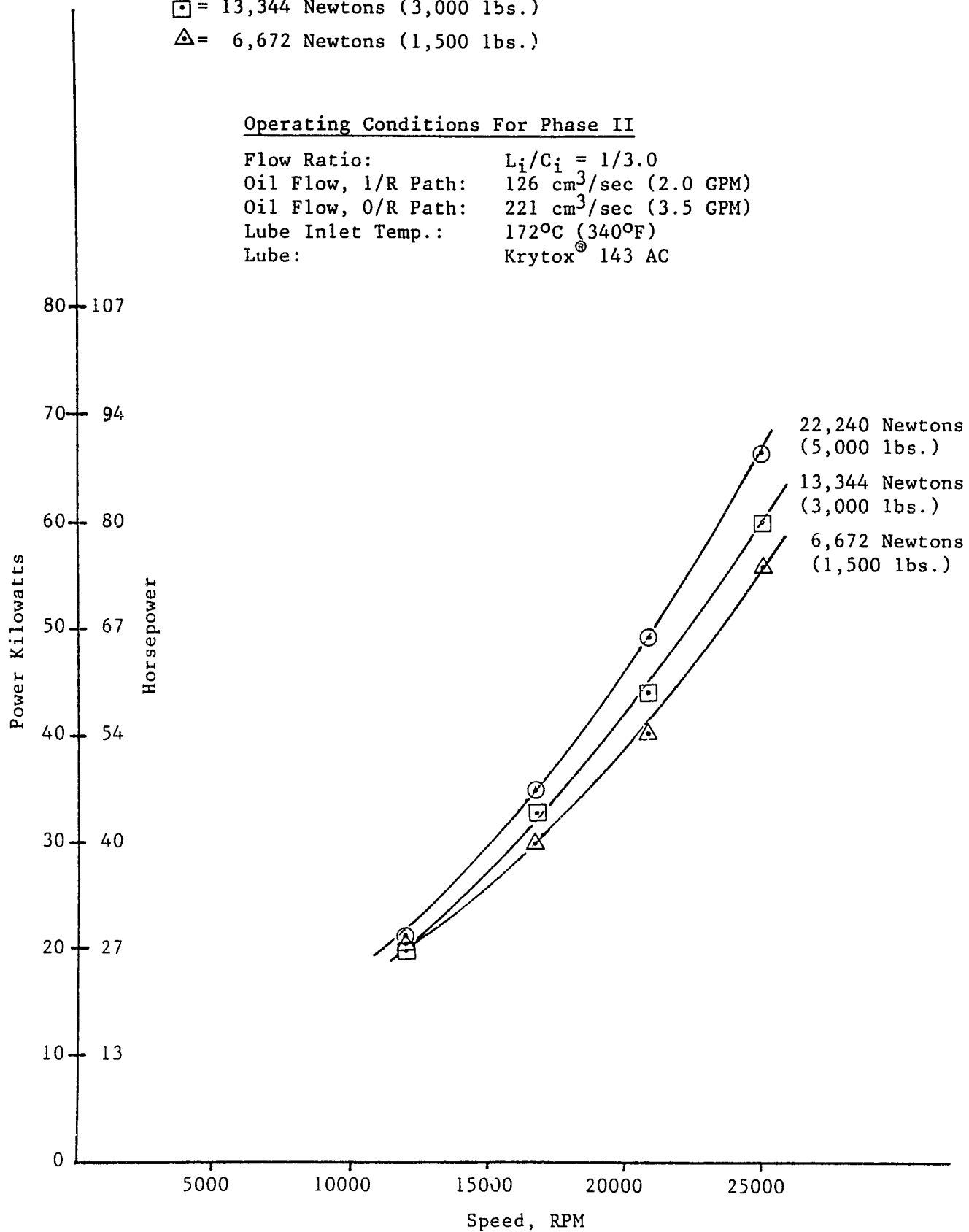


Figure 34. Bearing Power vs. Speed at Various Loads.

2. The bearing race temperatures, the temperature gradients across the bearings and the power loss could be tuned and varied with load, speed and the lubricant flow rate.
3. The cooling flow to the outer races affected the outer race temperatures significantly, but had only a small effect on the inner race temperatures. The power loss due to the changes in the cooling oil flow to the outer race was insignificant.
4. Compared with the results of the bearing tests using a type II lubricant, the high density Krytox lubricant produced a significantly and probably unacceptable higher value of power requirements.
5. Short bearing life was obtained in bearing tests with the Krytox 143 AC in an air atmosphere. The primary mode of failure was corrosive surface fatigue (pitting) on the bearing raceway surfaces. The nickel plating at the separator contact surfaces showed heavy wear after short periods of time.

SECTION 4  
TASK IV - CBS 600 BEARING TESTS

4.1 INTRODUCTION

The low fracture toughness of current rolling-element bearing materials is a critical technical barrier to the operation of advanced high performance aircraft gas turbines. Because of significant tangential hoop stresses developed in bearing races at high rotational speeds, bearing raceways will fail in rapid fracture mode after the development of fatigue spalls. This mode of failure, raceway failure, has been dramatically demonstrated with the 120 mm AISI M50 bearings tested at  $3 \times 10^6$  DN as reported in (9).

One approach to mitigating this problem is to utilize case-carburized bearing raceways. Case carburized bearings have hard surfaces for good rolling contact fatigue life and relatively soft, ductile cores for fracture toughness. To evaluate the effectiveness of this approach, inner races made with a carburizing alloy, CBS 600, were assembled into 120 mm bearings. These bearings were then tested to study the failure characteristics at  $3 \times 10^6$  DN. The test conditions were identical to those used in the previous fracture demonstration tests of AISI M50 bearings (9). Additionally, endurance tests were performed to establish the life characteristics of CBS 600 bearings.

Consequently, Task IV was subdivided into two phases:

- Phase I. Fracture Demonstration Tests
- Phase II. Endurance Tests

4.2 TEST BEARINGS

The test bearings were ABEC-5 grade, 120 mm bore ball bearings with split inner races. These were identical to those used during the earlier  $3 \times 10^6$  DN tests, except the inner raceways were manufactured of CBS 600 case carburized material. The test conditions were also identical to those used in the  $3 \times 10^6$  DN tests.

The CBS 600 material was provided by NASA in a 102 mm (4 in.) diameter billet. The nominal chemical composition of CBS 600 is shown in Table VII. Six pairs of inner races were manufactured. The inner rings were then carburized and heat-treated as described in Tables VIII and IX.

Two test coupons were carburized and heat-treated for pre-production quality control. In spite of the successful results on the coupons, the carburized production rings showed a massive carbide network to a depth of approximately 0.2 mm (0.008 inch) from the surface as shown in Figure 35. It is believed that the carbide network problem was caused by improper control of the carburizing atmosphere where surface carbon levels were in excess of 1.05%.

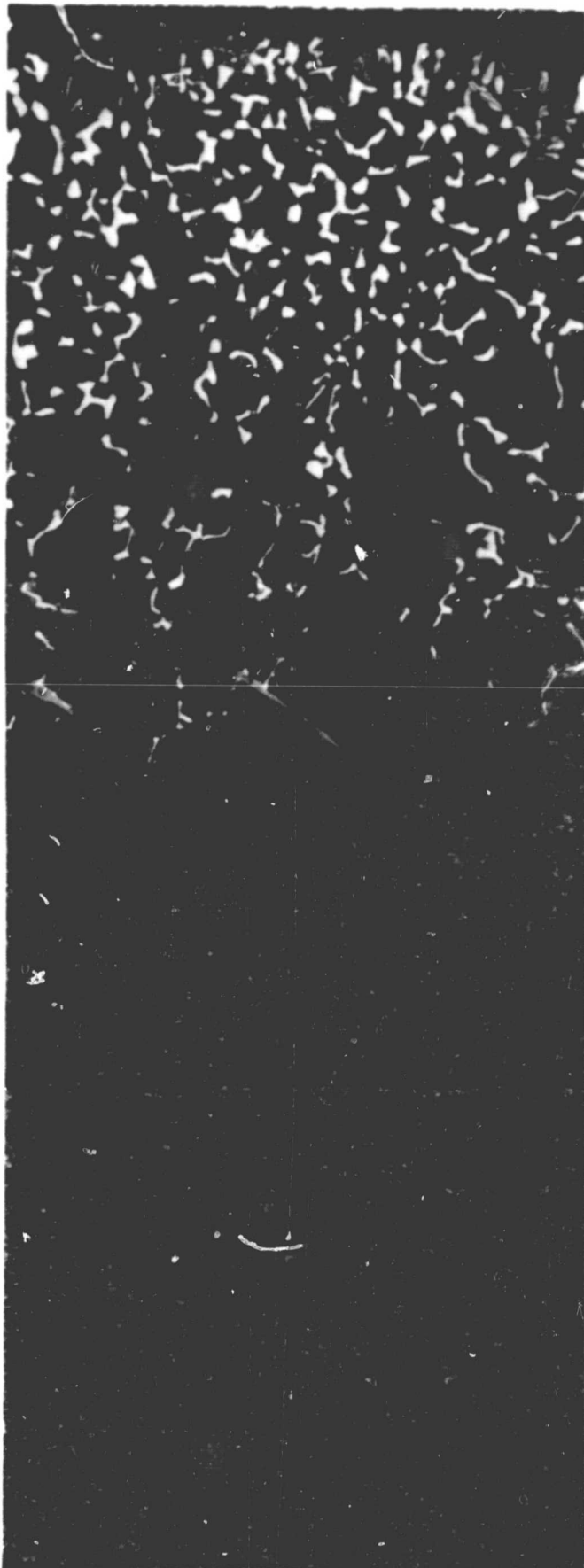


Figure 35. Massive Carbide Network  
in CBS 600 Inner Race  
After Carburizing at  
940.6°C (1725°F) for 11  
Hours.

Etchant: Nital

Mag.: 500X

ORIGINAL PAGE  
BLACK AND WHITE PHOTOGRAPH

TABLE VII

Nominal Chemical Composition of CBS 600

<u>Elements</u>	<u>Weight Percent</u>
Carbon	0.20
Manganese	0.60
Silicon	1.1
Chromium	1.5
Molybdenum	1.0
Iron	Balance

TABLE VIII

Forging Procedures for CBS 600 Bearing Races

- 1) Material to be heated to  $1260^{\circ}\text{C}$  ( $2300^{\circ}\text{F}$ ) and upset forged to height of 57.2 mm (2.25").
- 2) Forged blank will be hot pierced to form a 50.8 mm (2.00") I.D. at not less than  $1149^{\circ}\text{C}$  ( $2100^{\circ}\text{F}$ ) and reheated to  $1260^{\circ}\text{C}$  ( $2300^{\circ}\text{F}$ ).
- 3) Pierced blank will be mandrel saddled to an O.D. of 158.8 mm (6.25") with I.D. of 4.125" maintaining height of 57.2 mm (2.25").
- 4) Forging will be slow cooled in mica to room temperature.
- 5) Forgings will be reheated to  $732^{\circ}\text{C}$  ( $1350^{\circ}\text{F}$ ) and held for 2 hours, then cooled to room temperature in mica.

TABLE IX

Heat Treating Procedure for CBS 600

- Carburize at  $940.6^{\circ}\text{C}$  ( $1725^{\circ}\text{F}$ ) for 11 hours and oil quench.
- Heat to  $662.8^{\circ}\text{C}$  ( $1225^{\circ}\text{F}$ ) for 4 hours and slow cool.
- Austenitize at  $832.2^{\circ}\text{C}$  ( $1530^{\circ}\text{F}$ ) for 0.5 hours and oil quench.
- Deep freeze at  $-73.3^{\circ}\text{C}$  ( $-100^{\circ}\text{F}$ ) for 2.5 hours.
- Double temper at  $316^{\circ}\text{C}$  ( $600^{\circ}\text{F}$ ) for 2 plus 2 hours.

Since the forged rings did not have sufficient extra stock to permit removal of the layer containing the carbide network and because the massive carbide network was not acceptable for the Phase II endurance test program, it was decided to subject those rings, intended for life-testing, to an additional heat-treat cycle in an attempt to attenuate the carbide network. The balance of the races were processed without the additional heat-treat cycle because these parts were to be used for the fracture demonstration tests where fatigue life performance was not an important factor.

To eliminate the undesirable massive carbides, diffusion cycle experiments were performed on several pieces cut from a fully-processed CBS 600 inner race. The pieces were heated at 982°C (1800°F) and 1010°C (1850°F) for two hours each and rapid-cooled in a vacuum furnace and then reheat treated using the original austenitizing and tempering cycle. It was found that the massive carbide networks apparently disappeared after the diffusion cycles. This is shown in Figures 36 and 37.

Figure 38 shows the hardness gradient of a CBS 600 sample after the diffusion treatment. As shown, the 1010°C (1850°F) diffusion cycle increased the effective case depth by 0.76 mm (0.030 inch) while the 982°C (1800°F) increased case depth only a negligible amount. Based on this, the 982°C (1800°F) diffusion cycle was selected for the inner rings.

#### 4.2.1 Induced Defect

An artificial defect was generated in two inner ring raceways using electrical discharge machining. The procedures and dimensions of these defects were identical to those employed in the previous test program with AISI M50 bearings as described in (9).

### 4.3 RESULTS AND DISCUSSION

#### 4.3.1 Phase I - Fracture Demonstration Tests

A bearing assembled with a CBS 600 inner race with an induced defect and M50 balls and outer race was installed in the high speed, fatigue tester. The bearing was run at 25,000 rpm (3 million DN) with a thrust load of 22,240 Newtons (5,000 lbs.). A bearing race temperature of 216°C (420°F) was maintained. The lubricant (SATO 7730 per spec. MIL-L-23699) was introduced in the same manner and at the same rate of flow as defined in the 3 million DN fatigue test program performed earlier (9).

An inner race failure occurred after 0.65 hours of test. This failure did not initiate at the induced defect. Two spalls, 19.1 mm (0.75 inch) long and 12.7 mm (0.5 inch) long were observed as shown in Figure 39. Shortly after the spalling occurred, the tester shut down since the normal safety shut-off systems were operative.

ORIGINAL PAGE  
BLACK AND WHITE PHOTOGRAPH

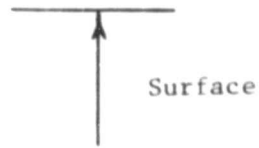
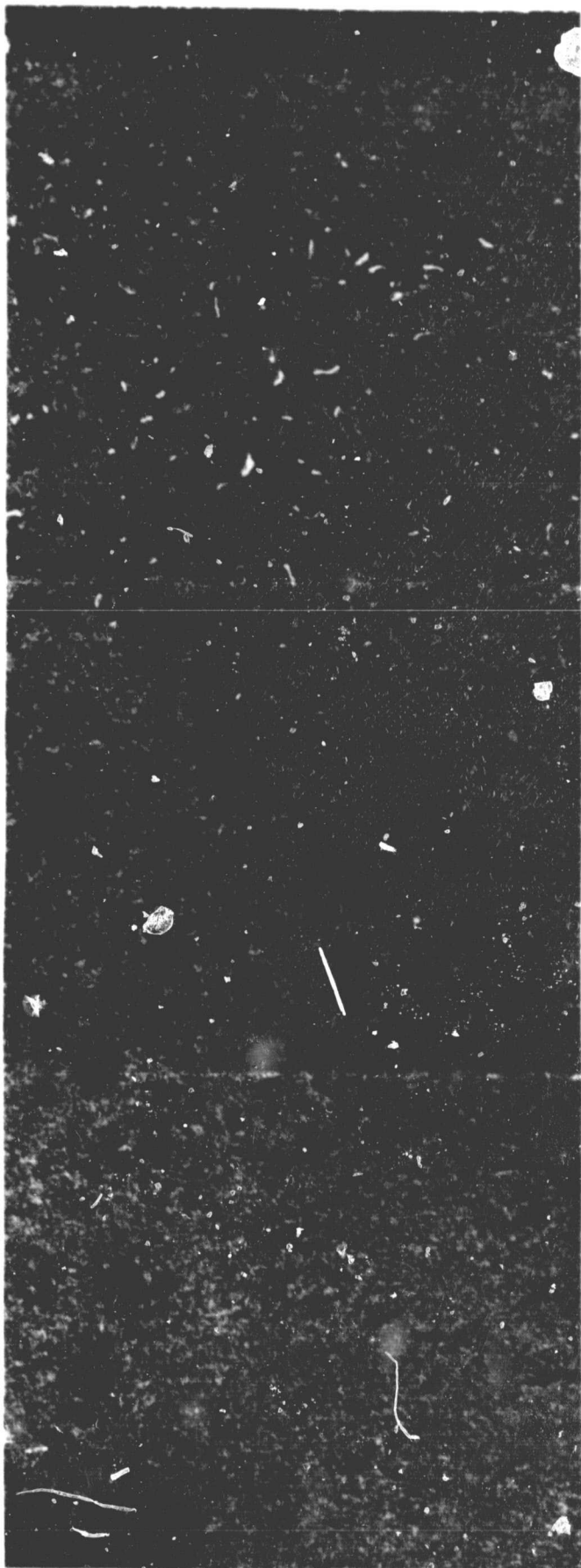
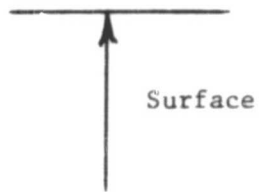


Figure 36. Microstructure of Carburized  
CBS 600 After a Diffusion  
Heat Treat Cycle at  $982^{\circ}\text{C}$   
( $1800^{\circ}\text{F}$ ) for 2 Hours in  
Vacuum.

Etchant: Nital

Mag.: 500X



ORIGINAL PAGE  
BLACK AND WHITE PHOTOGRAPH

Figure 37. Microstructure of Carburized  
CBS 600 After a Diffusion  
Heat Treat Cycle at  $1010^{\circ}\text{C}$   
( $1850^{\circ}\text{F}$ ) for 2 Hours in  
Vacuum.

Etchant: Nital.

Mag.: 500X

ORIGINAL PAGE IS  
OF POOR QUALITY

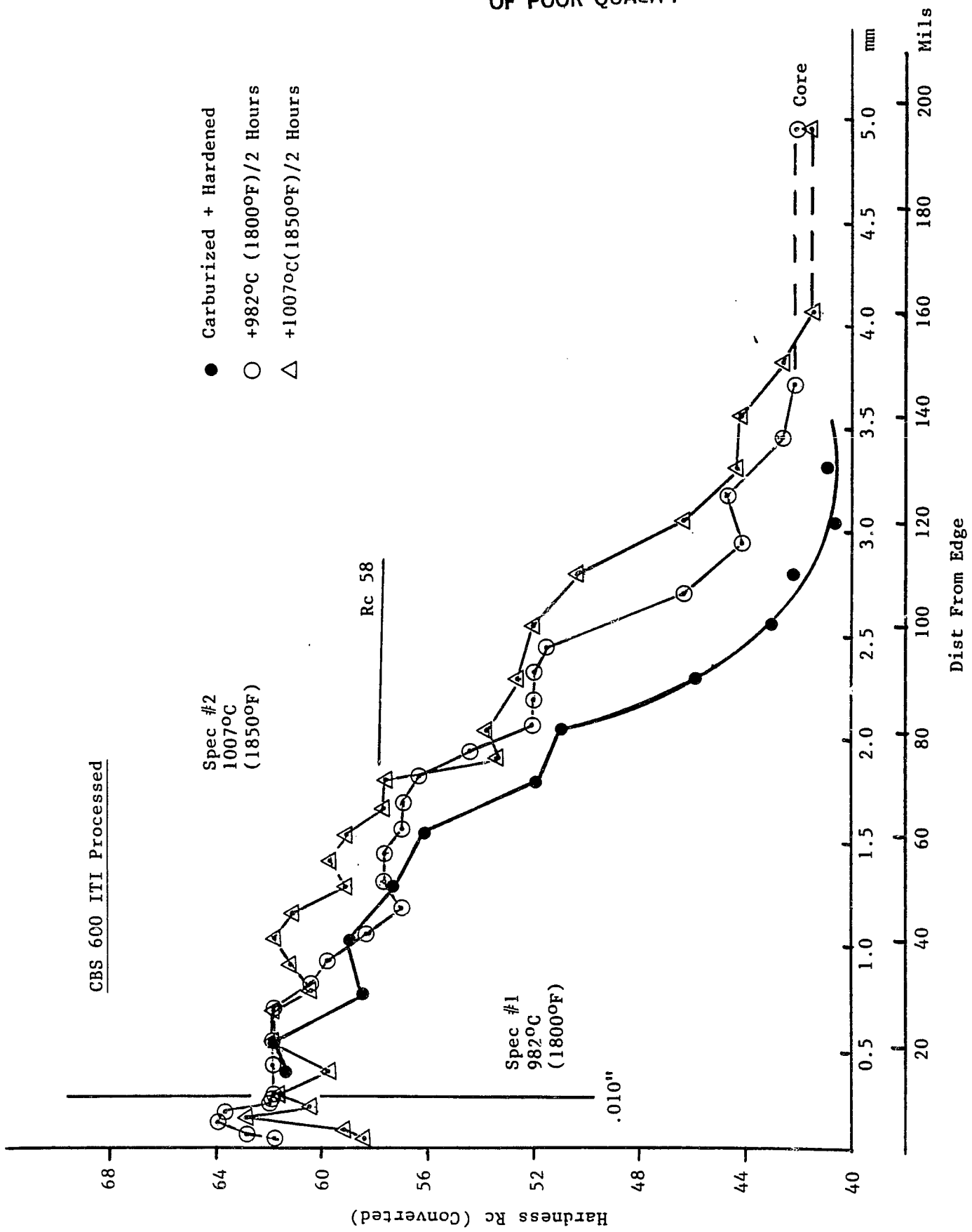


Figure 38. Hardness Gradient in CBS 600 After Carburization and 1010°C (1850°F) Diffusion Heat Treatment in Vacuum for 2 Hours.

ORIGINAL PAGE  
BLACK AND WHITE PHOTOGRAPH

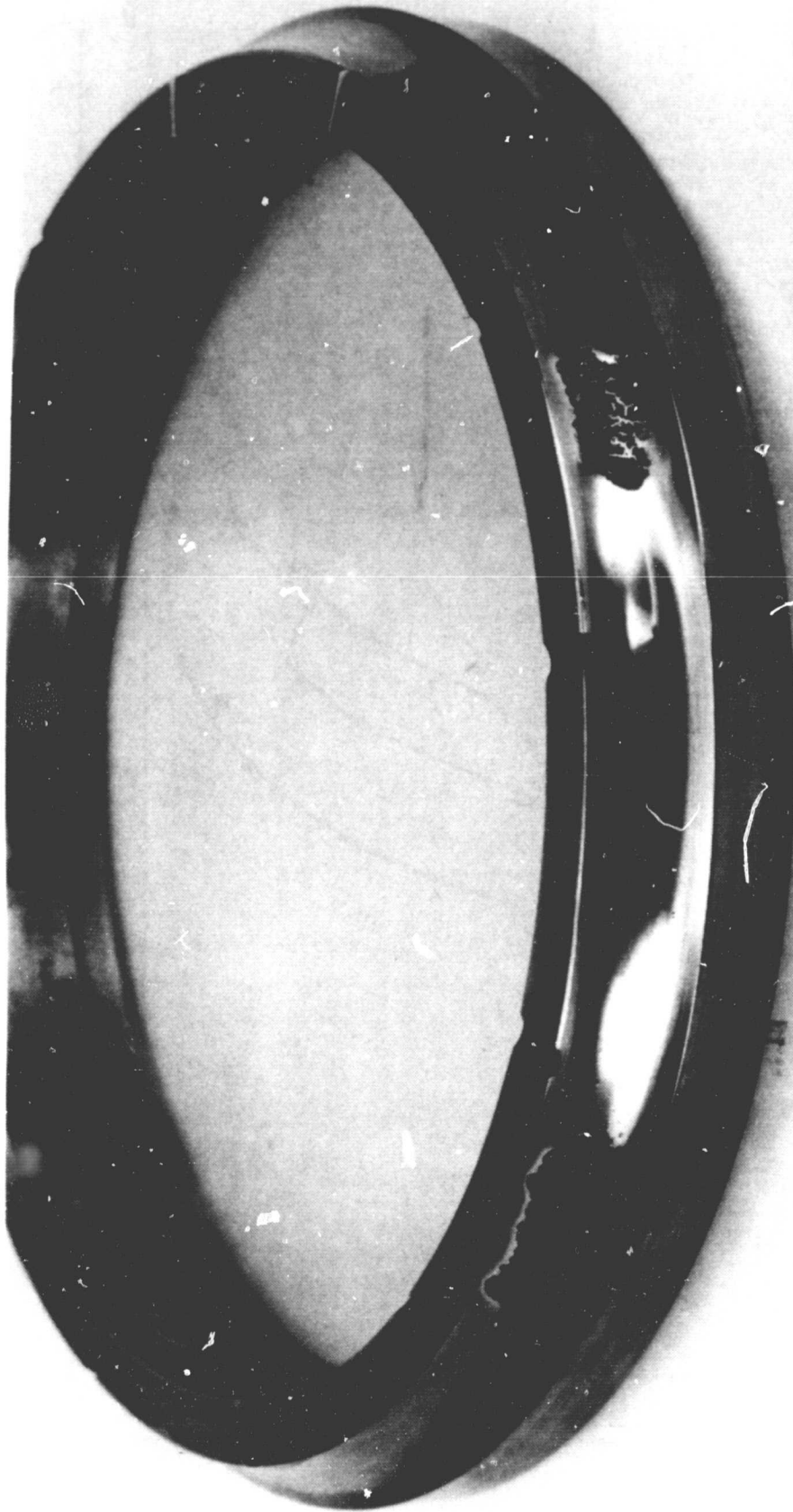


Figure 39. Premature Inner Race Failures in Bearing S/N 5 After 0.65 Hours Testing. (Failures did not occur at the induced defect.)

The second bearing with an induced defect was installed and run under the identical conditions as described above, except that all tester safety shut-off devices were disconnected to allow continuation of the test after the initiation of a spalling failure. This bearing was run for 3.5 hours before the expected inner race failure developed. The test was continued, although the cooling flow rate had to be increased to prevent overheating of the bearing. After 24.7 minutes of operating with the spall, the drive power demand exceeded the motor capacity, tripping the drive motor overload. Restarting the tester was not successful and the test was terminated.

For comparison, the bearing test with a through-hardened AISI M50 ring performed in an earlier program had developed a normal spall failure from the artificially induced defect after 6 hours, 17 minutes of testing time, and had fractured into eight discrete segments 7.5 minutes after the initiation of a spalling failure under the identical test conditions used in this study.

Despite the fact that the inner rings had less than optimum microstructure, the present test results indicate that a 120 mm ball bearing inner race, manufactured of a case carburized material can withstand continued high load, high speed operation without raceway fracture after a fatigue spall has developed.

Post-test examination confirmed that the inner race spalling failure was initiated at the artificial defect. An overall view of the failed bearing is shown in Figure 40. The continued running resulted in a spall extending over approximately 40% of the entire race circumference as shown in Figure 41. The location of the induced defect was found in the spalled area and 10.2 mm (0.4 inch) from the leading edge of the spall, indicating the spalling had also typically propagated against the ball rolling direction. There was only minor secondary damage to the other bearing components, and the structural integrity of the spalled inner race had been fully maintained.

#### 4.3.2 Phase II - Endurance Tests

The objective of this portion of the program was to demonstrate the rolling contact fatigue life of CBS 600 bearing material. Previous laboratory tests using NASA four ball testers (12) and GE RC rigs (13) showed that the rolling contact fatigue life of CBS 600 was equivalent to that of AISI M50. 120 mm bearings were assembled with CBS 600 inner rings. The remaining components of the bearings were identical to those used in the previous full scale  $3 \times 10^6$  DN tests. The endurance tests were performed at 25,000 rpm ( $3 \times 10^6$  DN) with 22,240 Newtons (5,000 lbs.) thrust load. Three tests were conducted, each resulting in an early failure of 1.4 hours (S/N 3), 3.3 hours (S/N 4) and 1.5 hours (S/N 6). These are all quite premature failures, as was the failure of the test bearing in the earlier fracture demonstration test. Figures 42 and 43 show typical spalling failures observed in the CBS 600 inner rings.

The short lives obtained with all the CBS 600 inner races, strongly suggest that the material may have been improperly processed. To confirm this, a detailed metallographic examination was made on the failed raceways.

ORIGINAL PAGE  
BLACK AND WHITE PHOTOGRAPH

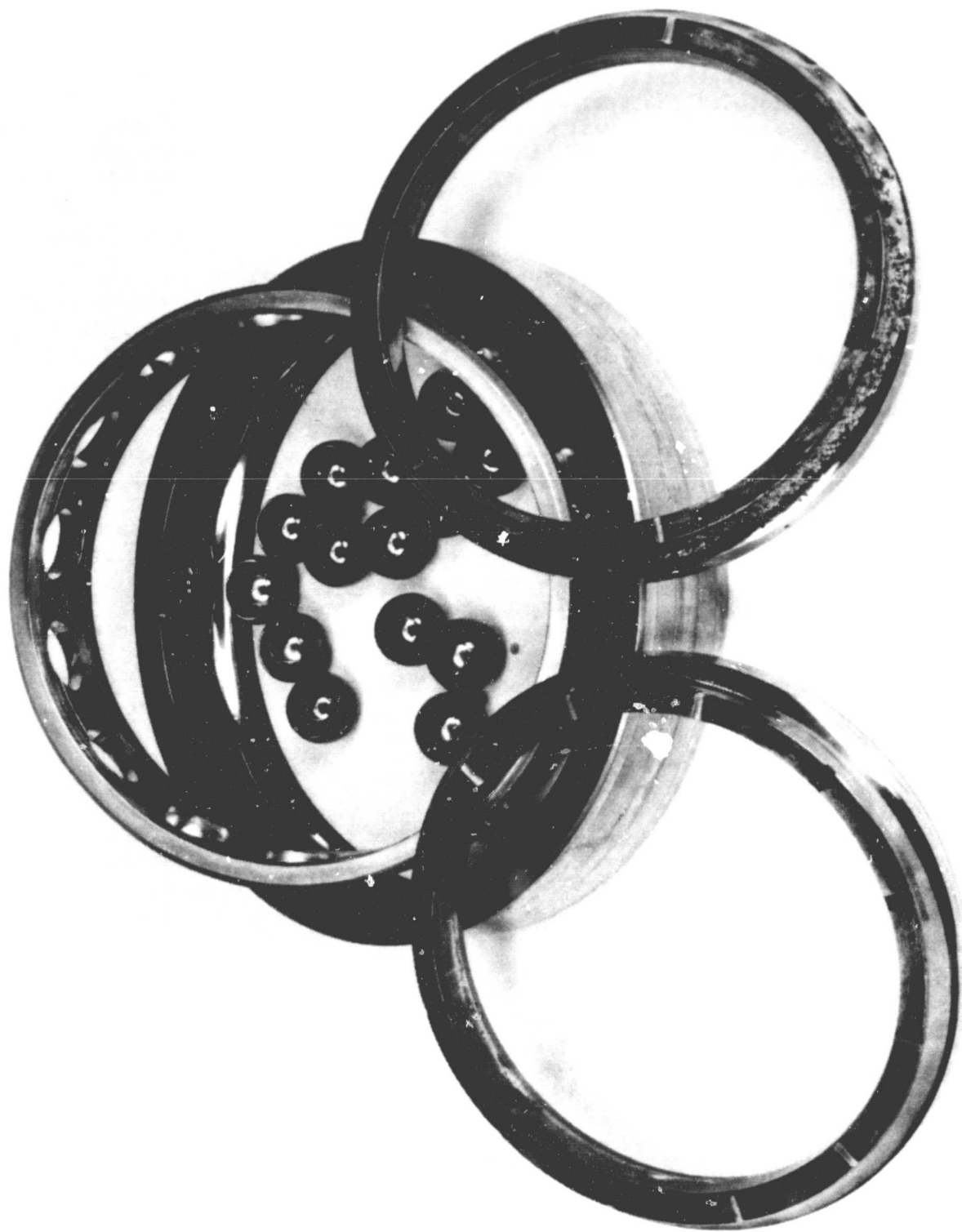


Figure 40. Overall View of Failed Bearing S/N 2 which was Operated for 24.7 Minutes After Spalling Failure.

ORIGINAL PAGE  
BLACK AND WHITE PHOTOGRAPH



Figure 41. CBS 600 Inner Race of Bearing S/N 2 After Extended Running Following Initial Spalling Failure.

ORIGINAL PAGE  
BLACK AND WHITE PHOTOGRAPH

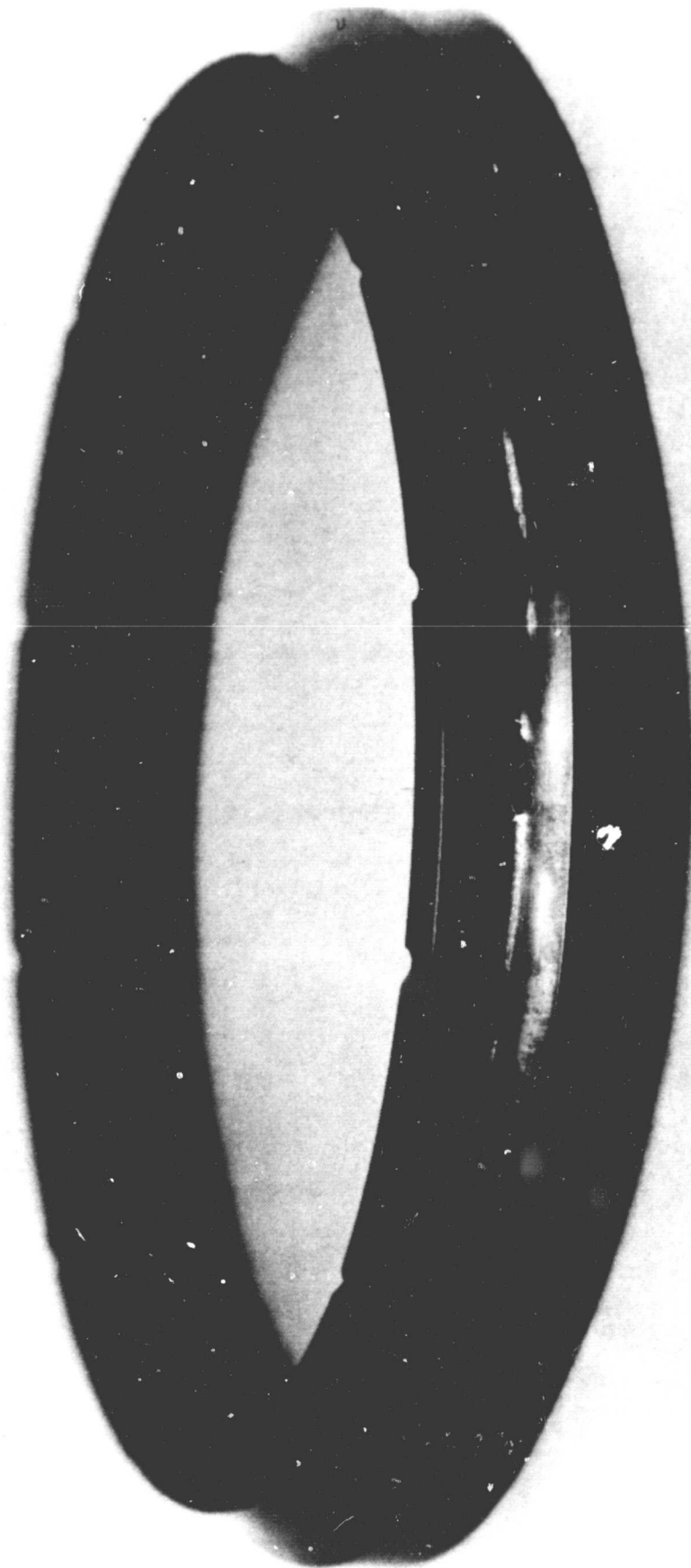


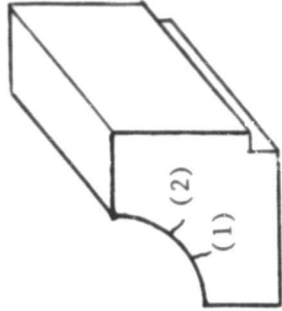
Figure 42. Typical Spalling Fatigue Failure on CBS 600  
Inner Rings on Bearing S/N 3.

ORIGINAL PAGE  
BLACK AND WHITE PHOTOGRAPH

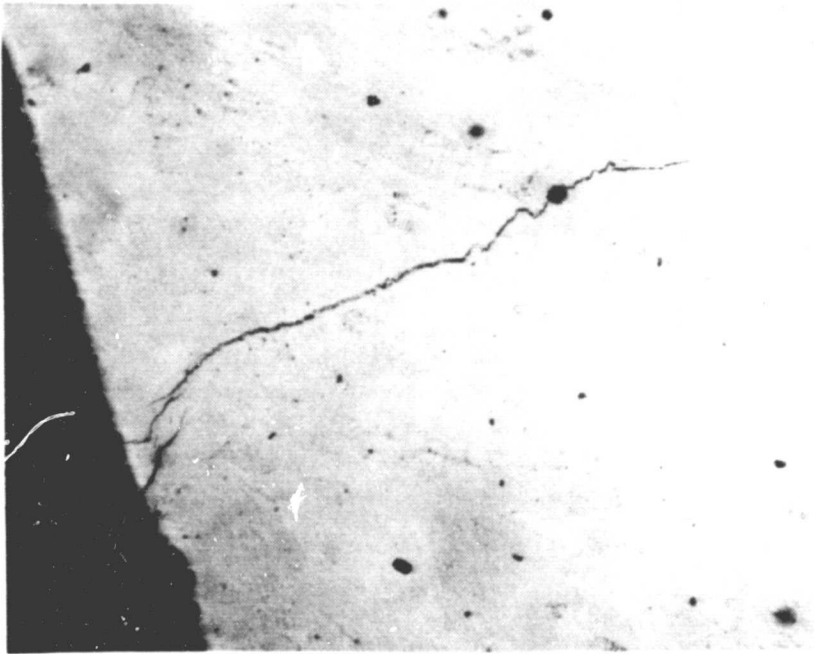


Figure 43. Typical Spalling Fatigue Failure on CBS 600  
Inner Rings of Bearing S/N 4.

ORIGINAL PAGE  
BLACK AND WHITE PHOTOGRAPH



Crack Location (2)



Crack Location (1)

Figure 44. Cross Sectional View of Cracks in  
CBS 600 Inner Races from Bearing  
S/N 6.

Mag.: 50X

Etchant: None.

Each failed ring was cross-sectioned perpendicular to the circumferential rolling direction in a number of locations, particularly near the spalled region. Metallographic mounts were prepared and examined. A multiplicity of cracks emanating from the raceway surface and perpendicular to the rolling direction were found. Figure 44 illustrates a typical example of these cracks. The cracks exhibit the typical pattern normally encountered with quench cracks. This type of processing defect will undoubtedly lead to a premature failure.

It is likely that these defects formed during the cooling cycle after carburizing. The CBS 600 inner rings were rapid quenched into oil following the procedure recommended by the manufacturer of this alloy. Normally, most carburized parts are slow cooled after carburizing. When a rapid cool from the carburizing temperature is used, the parts must be stress-relieved within a short period of time.

This is also true with the hardening, or austenitizing, process. Tempering cycles must be followed immediately after the austenitizing. In the case of the CBS 600 rings, it is known that the elapsed time between quenching for the carburizing cycle and the subsequent stress-relief exceeded the allowable time limit.

It is unfortunate that because of time and money restrictions, the CBS 600 life testing could not be repeated.

#### 4.4 TASK IV CONCLUSIONS

Inner races were manufactured with case-carburized CBS 600 material and assembled into the 120 mm bore ball bearings with split inner rings. The bearings were tested at 25,000 rpm ( $3 \times 10^6$  DN) with a thrust load of 22,240 Newtons (5,000 lbs.) in the fatigue tester. The test conditions were identical to those used in the previous tests (9). The following conclusions were reached:

- 1) It was indicated that a 120 mm ball bearing inner race, manufactured of a CBS 600 case carburized material can withstand continued high speed, high load operation without experiencing rapid fracture after a fatigue spall has developed.
- 2) In the endurance tests of bearings assembled with the CBS 600 inner races, all inner races failed within four hours of testing time in four tests. These premature failures were attributed to processing defects formed during the heat-treat cycle.

SECTION 5  
REFERENCES

1. Bamberger, E.N., "Bearing Fatigue Investigations", NASA CR 72290, Final Engineering Report, NASA Contract NAS3-7261, September, 1967.
2. Bamberger, E.N., "Bearing Fatigue Investigation", NASA CR 134621, NASA Contract NAS3-11148, June, 1974.
3. Parker, R.J., Bamberger, E.N., and Zaretsky, E.V., "Evaluation of Lubricants for High-Temperature Ball Bearing Applications", Journal of Lubrication Technology, Trans. ASME. Series F. Volume 90. No. 1, January, 1968.
4. Bamberger, E.N., Zaretsky, E.V., and Anderson, W.J., "Fatigue Life at 120 mm Bore Ball Bearings at 600°F with Fluorocarbon, Polphenylether and Synthetic Paraffinic Base Lubricants", NASA TN-D4850, 1968.
5. Bamberger, E.N., Zaretsky, E.V., and Anderson, W.J., "Effect of Three Advanced Lubricants on High Temperature Bearing Life", Journal of Lubrication Technology, Trans. ASME. Series F. Vol. 92. No. 1. January, 1970, pp a3-33.
6. Zaretsky, E.V., Anderson, W.J., and Bamberger, E.N., "Rolling Element Bearing Life from 400°F to 600°F", NASA TN D-5002, 1969.
7. Signer, H., Bamberger, E.N., and Zaretsky, E.V., "Parametric Study of the Lubrication of Thrust Loaded 120 mm Bore Ball Bearings to 3 Million DN", ASME Transactions, Journal of Lubrication Technology, Volume 96, Series F, No. 3, July, 1974.
8. Bamberger, E.N., Zaretsky, E.V., and Signer, H., "Effect of Speed and Load on Ultra-High-Speed Ball Bearings", NASA TN D-7870, January, 1975.
9. Bamberger, E.N., Zaretsky, E.V., and Signer, H., "Endurance and Failure Characteristics of Main Shaft Jet Engine Bearings at  $3 \times 10^6$  DN", ASME Transactions, Journal of Lubrication Technology, Volume 98, Series F, No. 4, October, 1976.
10. Dolle, R.E., Harsacky, F.J., Schwenker, H., and Adamczak, R.L., "Chemical, Physical and Engineering Performance Characteristics of a New Family of Perfluorinated Fluids", Technical Report AFML-TR-65-358, September, 1965.
11. Dolle, R.E. and Harsacky, F.J., "New High Temperature Additive Systems for PR-143 Fluids", Technical Report AFML-TR-65-349, January, 1966.
12. Townsend, D.P. and Zaretsky, E.V., "Endurance and Fatigue Characteristics of Modified Vasco X-2, CBS 600 and AISI 9310 Spur Gears", ASME Paper 80-C2/DET-58, 1980.
13. Nahm, A.H., "Rolling Element Fatigue Testing of Gear Materials", NASA Contract Report CR-135450, June, 1978.